SU(2) formulation of the t-J model: Application to underdoped cuprates

Patrick A. Lee
Department of Physics, Massachusetts Institute of Technology, Cambridge, Massachusetts 02139

Naoto Nagaosa
Department of Applied Physics, University of Tokyo, Tokyo 113, Japan

Tai-Kai Ng
Department of Physics, Hong Kong University of Science and Technology, Clearwater Bay, Hong Kong

Xiao-Gang Wen
Department of Physics, Massachusetts Institute of Technology, Cambridge, Massachusetts 02139
(Received 22 January 1997)

We develop a slave-boson theory for the t-J model at finite doping that respects an SU(2) symmetry: a symmetry previously known to be important at half filling. The mean-field phase diagram is found to be consistent with the phases observed in the cuprate superconductors, which contain d-wave superconductor, spin-gap, strange metal, and Fermi-liquid phases. The spin-gap phase is best understood as the staggered flux phase, which is nevertheless translationally invariant for physical quantities. The physical electron spectral function shows small Fermi segments at low doping that continuously evolve into the large Fermi surface at high-doping concentrations. The close relation between the SU(2) and the U(1) slave-boson theory is discussed. The low-energy effective theory for the low-lying fluctuations is derived and additional lying modes [which were overlooked in the U(1) theory] are identified. [S0163-1829(98)08109-0]

I. INTRODUCTION

It is well established that high-temperature superconductivity appears in cuprates when holes are doped into the parent compound, which is understood to be Mott-Hubbard antiferromagnetic (AF) insulators. Since the parent compound is insulating only by virtue of strong correlation, it stands to reason that a strongly correlated model is the requisite starting point to describe the cuprates. The simplest such model is the two-dimensional t-J model and a large effort has been made to study how the phase diagram evolves from a Heisenberg antiferromagnet when a concentration x of holes is introduced. The doping of a Mott-Hubbard insulator is a relatively new problem in condensed-matter physics and involves issues quite different from the doping of a band insulator. A key question is the evolution of the Fermi surface with doping. At low doping, the unit cell is doubled in the AF state and the first holes will form small pockets, not unlike the doping of band insulators. The pockets are centered at $(\pi/2,\pi/2)$.[1] On the other hand, when the hole concentration is large, it is known that a large Fermi surface is formed, with an area given by $1-x$, in agreement with Luttinger theorem.[2] The point is that the local moments on the copper are now counted as part of the conduction electron that makes up the Fermi sea. The key question is how this evolution takes place as a function of doping. It seems quite likely that the state for intermediate doping may contain features not encountered before. Indeed, concepts such as quantum spin liquid states and spin-charge separation were introduced early on and much work has gone into the development of a formal theory that exhibits some of these features.[3] One line of approach is to start from mean-field decoupling[4–7] and study fluctuations about the mean-field solution, which turns out to be a U(1) gauge theory.[8–10] On the experimental front, much work has focused on the underdoped region, defined as the region of hole concentration between the onset of superconductivity and the maximal T_c, because many anomalous properties are found in the metallic state in this regime. For example, unlike optimally doped systems where the magnetic susceptibility χ and the Knight shift are temperature independent, underdoped cuprates generally show a reduction in χ below 400 K or so.[11] At the same time the specific heat is found to be suppressed relative to the T linear behavior expected for conventional metals.[12] This behavior suggests the formation of a gap in the excitation spectrum. This gap also shows up in the c-axis frequency-dependent conductivity,[13] but the conductivity in the plane is not so strongly affected. The in-plane dc conductivity shows a suppression below about 200 K relative to the linear T resistivity observed at higher temperatures. This suppression can be attributed to a reduction of the width of the Drude-like peak by a factor of 2 with little effect on the spectral weight.[14] The reduction of the conductivity is due to the scattering rate rather than to the carrier concentration.[15] These observations suggest that the gap appears only in the spin and not the charge degrees of freedom in the two-dimensional plane and has been loosely referred to as the spin gap. We should add that the strongest gaplike behavior has been seen in the Cu NMR relaxation rate and in neutron scattering, both of which are sensitive to spin excitation at momentum $Q=(\pi,\pi)$. This latter phenomenon usually starts at a lower temperature of order 200 K and it has been argued that it is observed only in bilayer or trilayer materials.[11,16] We shall take the point of view that the behav-

 © 1998 The American Physical Society

ior at (π,π) may be a more delicate issue depending on nesting properties at the Fermi surface, etc., and for the rest of the paper we shall use the term ''spin gap'' to refer to properties mentioned earlier that are characteristic of single-layer as well as multilayer cuprates.

Very recently, angle-resolved photoemission experiments have yielded important information concerning the electronic excitations of underdoped cuprates. It was discovered that a gap in the spectral functions already existed in the normal state.[17,18] Furthermore, the size of this gap and its dependence on $\vec{k}$ space is similar to the d-wave-type gap observed in the superconducting state. The difference is that in the normal state, the gap appears to close in a finite segment near $(\pi/2,\pi/2)$, leaving a ''Fermi-surface segment.'' If this energy gap is related to the spin gap, this observation gives an important boost to the notion of spin-charge separation. This is because when an electron is removed from the plane, as in photoemission and in c-axis conductivity, one is forced to pay the energy cost to break the singlet pairs in the plane, whereas for in-plane conductivity, charge transport may occur within the spin singlet sector. Such a behavior is in fact a natural consequence of the mean-field phase diagram of the t-J model that has been in existence for some time.[6,7] In this theory the constraint of no double occupancy is enforced by writing the electron operator $c_{\alpha i}$ in terms of auxiliary fermions and boson particles $c_{\alpha i}=f_{\alpha i}b_i^\dagger$ and demanding that each site is occupied by either a fermion or a boson. In a mean-field treatment, the order parameters $\chi_{ij}=\langle f_{\alpha i}^\dagger f_{\alpha j}\rangle$ and $\Delta_{ij}=\langle f_{1i}f_{2j}-f_{2i}f_{1j}\rangle$ describe the formation of singlets envisioned in Anderson's resonating valence-bond (RVB) picture.[3] Above the Bose condensation temperature of the bosons, spin charge separation occurs at the mean-field level. In particular, in the underdoped regime the fermions are paired in a d-wave state, leading to a gap in the spin excitation but no gap in the charge excitation. This scenario has been used as an explanation of the spin-gap phenomenon.[19,20]

While the conventional U(1) mean-field theory has many attractive features, it suffers from a number of defects. First, when an attempt was made to improve the theory by including gauge fluctuations, it was found that the d-wave state was unstable.[21] Second, in the underdoped regime, there are indications that the system is unstable to the spontaneous generation of gauge fluxes at finite wave vectors.[22] Such instabilities will lead to a breaking of translation symmetry that is not observed experimentally. We note that it has been suggested recently that a modified d-wave state with a large gap at the $(0,\pi)$ point and vanishing gap along a segment near $(\pi/2,\pi/2)$ may be stable against gauge fluctuations.[23] However, the question about finite wave-vector instabilities remains. Such considerations motivated us to produce a formulation of the constraint that generalizes the SU(2) theory for the half-filled t-J model to the t-J model away from half filling.[24] Our hope is that since SU(2) gauge symmetry is an exact symmetry at half filling, the mean-field approximation of our formulation may capture more accurately the low-energy degrees of freedom and may be a better starting point for small x. Indeed, we found that in the underdoped region, the mean-field solution may be understood as a d-wave pairing state, or equivalently as a staggered-flux (s-flux) phase, where the gauge flux alternates on even or odd sublattices. These states are related by local SU(2) gauge transformations and do not break translational symmetry. Furthermore, these states are connected smoothly to the π-flux phase at half filling that has large excitation energy at the $(0,\pi)$ point, comparable to that at (0,0). This is in agreement with photoemission experiments on the insulating cuprates, suggesting that the AF state may resemble the π-flux phase at short distances.[25,26] Furthermore, in the experiment the state at $(0,\pi)$ moves towards the Fermi surface with doping, which can be understood in the mean-field theory as a gradual closing of the spin gap. In this work[24] we also introduced a residual attraction between the boson and fermions and show that this gives to Fermi-surface segments near the $(\pi/2,\pi/2)$ point that grows with doping. Thus the SU(2) mean-field theory allows us to answer the fundamental question of how the Fermi surface evolves from hole pockets near the $(\pi/2,\pi/2)$ point near half filling to a large Fermi surface for large-doping concentration.

In this paper we give a more detailed description of the SU(2) theory and we also offer an alternative formulation that has some advantage over the original SU(2) mean-field theory, particularly in the approach to large doping. More specifically, in Sec. II we show that the SU(2) theory is intimately related to the original U(1) theory. This leads us to a formulation in terms of a σ model of slowly varying boson fields. This is discussed in Secs. III and IV. In Sec. V we present detailed calculations of the electron spectral function, comparing the original SU(2) mean-field approach and the present σ-model formulation. We also made some modifications of the interaction potential between fermions and bosons, which lead to considerable improvement of the spectral function when compared with experiments. In Sec. VI we discuss the collective excitations of the theory, which are SU(2) gauge fields, and we point out the important massless gauge fields in different parts of the phase diagram. In particular, the existence of a massless mode in the staggered flux phase is an important feature of the SU(2) theory compared to the U(1) formulation. We also briefly discuss the response to an electromagnetic field of the normal and superconducting states.

II. RELATION OF THE SU(2) FORMULATION TO U(1) THEORY

Affleck *et al.*[27] pointed out that the t-J model at half filling obeys an exact SU(2) symmetry. They introduced the SU(2) doublets

$$\psi_{1i}=\begin{pmatrix} f_{1i} \\ f_{2i}^\dagger \end{pmatrix}, \quad \psi_{2i}=\begin{pmatrix} f_{2i} \\ -f_{1i}^\dagger \end{pmatrix} \tag{1}$$

to represent the destruction of a spin up and spin down on site i, respectively. This expresses the physical idea that a physical up spin can be represented by an up-spin fermion or the absence of a down-spin fermion once the constraint is imposed. The theory is invariant under the local transformation $\psi_{\alpha i}\rightarrow g_i\psi_{\alpha i}$, where g is a 2×2 matrix representation of the SU(2) group. In the original formulation, which we shall refer to as the U(1) theory, this symmetry is broken upon the introduction of holes.

In Ref. 24 a formulation of the constraint of no double occupation in the t-J model was introduced that preserves the SU(2) symmetry even away from half filling. The key step is the introduction of a doublet of bosons

$$h_i=\begin{pmatrix} b_{1i} \\ b_{2i} \end{pmatrix} \tag{2}$$

on each site, so that the physical electron operator can be written as an SU(2) singlet, i.e.,

$$c_{1i}=\frac{1}{\sqrt{2}}h_i^\dagger\psi_{1i}=\frac{1}{\sqrt{2}}(b_{1i}^\dagger f_{1i}+b_{2i}^\dagger f_{2i}^\dagger),$$

$$c_{2i}=\frac{1}{\sqrt{2}}h_i^\dagger\psi_{2i}=\frac{1}{\sqrt{2}}(b_{1i}^\dagger f_{2i}-b_{2i}^\dagger f_{1i}^\dagger). \tag{3}$$

The t-J Hamiltonian

$$H=\sum_{\langle i,j\rangle}[J(\vec{S}_i\cdot\vec{S}_j-\tfrac{1}{4}n_in_j)-t(c_{\alpha i}^\dagger c_{\alpha j}+\text{H.c.})] \tag{4}$$

can now be written in terms of our fermion-boson (FB) fields. The Hilbert space of the FB system is larger than that of the t-J model. However, the local SU(2) singlets satisfying $(\frac{1}{2}\psi_{\alpha i}^\dagger\vec{\tau}\psi_{\alpha i}+b_i^\dagger\vec{\tau}b_i)|\text{phys}\rangle=0$ form a subspace that is identical to the Hilbert space of the t-J model. On a given site, there are only three states that satisfy the above constraint. They are $f_1^\dagger|0\rangle$, $f_2^\dagger|0\rangle$, and $1/\sqrt{2}(b_1^\dagger+b_2^\dagger f_2^\dagger f_1^\dagger)|0\rangle$ corresponding to a spin-up electron, and a spin-down electron, and a vacancy, respectively. Furthermore, the FB Hamiltonian, as a SU(2) singlet operator, acts within the subspace and has the same matrix elements as the t-J Hamiltonian. The projection to the physical subspace is accomplished by introducing a set of three auxiliary fields a_{0i}^ℓ, $\ell=1,2,3$, on each site i. The partition function is written after a standard Hubbard-Stratonovich transformation as

$$Z=\int Dh\ Dh^\dagger D\psi\ D\psi^\dagger D\vec{a}_0 DU\ \exp\left(-\int_0^\beta\widetilde{L}\right), \tag{5}$$

where the Lagrangian $\widetilde{L}$ is given by

$$\begin{aligned}\widetilde{L}=&\frac{\widetilde{J}}{2}\sum_{\langle ij\rangle}\text{Tr}[U_{ij}^\dagger U_{ij}]+\frac{1}{2}\sum_{i,j,\alpha}\psi_{\alpha i}^\dagger(\partial_\tau\delta_{ij}+\widetilde{J}U_{ij})\psi_{\alpha j}\\&+\sum_{i,\ell}a_{0i}^\ell\left(\frac{1}{2}\psi_{\alpha i}^\dagger\tau^\ell\psi_{\alpha i}+h_i^\dagger\tau^\ell h_i\right)\\&+\sum_{i,j}h_i^\dagger[(\partial_\tau-\mu)\delta_{ij}+\widetilde{t}U_{ij}]h_j.\end{aligned} \tag{6}$$

The matrix

$$U_{ij}=\begin{bmatrix}-\chi_{ij}^* & \Delta_{ij}\\ \Delta_{ij}^* & \chi_{ij}\end{bmatrix}, \tag{7}$$

where χ_{ij} represents fermion hopping and Δ_{ij} represents fermion pairing, respectively, and $\widetilde{J}=3J/8$, $\widetilde{t}=t/2$.[28] The density of physical holes equals the total density of bosons

$$\langle 1-c_{\alpha i}^\dagger c_{\alpha i}\rangle=\langle h_i^\dagger h_i\rangle=\langle b_1^\dagger b_1+b_2^\dagger b_2\rangle=x \tag{8}$$

and is enforced by the chemical potential μ.

The a_{0i}^ℓ enforces the local constraint

$$\langle\tfrac{1}{2}\psi_{\alpha i}^\dagger\tau^\ell\psi_{\alpha i}+h_i^\dagger\tau^\ell h_i\rangle=0. \tag{9}$$

In particular, for $\ell=3$ we have

$$\langle f_{\alpha i}^\dagger f_{\alpha i}+b_{1i}^\dagger b_{1i}-b_{2i}^\dagger b_{2i}\rangle=1. \tag{10}$$

The Lagrangian is invariant under the local SU(2) transformation

$$\begin{aligned}&\psi_{\alpha i}\to g_i^\dagger\psi_{\alpha i},\quad h_i\to g_i^\dagger h_i,\quad U_{ij}\to g_i^\dagger U_{ij}g_j,\\&a_{0i}^\ell\tau^\ell\to g_i^\dagger a_{0i}^\ell\tau^\ell g_i-g_i\partial_\tau g_i^\dagger,\end{aligned} \tag{11}$$

where $g_i(\tau)$ is a 2×2 matrix that represents an SU(2) group element.

Equations (5) and (6) are a faithful representation of the t-J model, just as the more standard U(1) representation is. The two representations must be equivalent, as long as we include all the fluctuations. To understand the relation between the SU(2) and the U(1) theory, we will rewrite the SU(2) theory to make it as similar to the U(1) theory as possible. In Appendix A we will do the reverse, i.e., we will start with the U(1) theory and write it in the form of the SU(2) theory; we will also discuss some subtleties of the relation.

The key ingredient is that the two-component boson field in the SU(2) representation is nothing but an SU(2) rotation of the standard slave boson b_i, i.e.,

$$h_i=g_i\begin{pmatrix} b_i \\ 0\end{pmatrix}. \tag{12}$$

The matrix g_i can be parametrized as

$$g_i=\begin{pmatrix} z_{i1} & -z_{i2}^* \\ z_{i2} & z_{i1}^*\end{pmatrix}, \tag{13}$$

with the constraint $\Sigma_\alpha z_{i\alpha}^* z_{i\alpha}=1$, which is satisfied by the parametrization

$$z_{i1}=e^{-i(\alpha/2)}e^{-i(\phi/2)}\cos\frac{\theta}{2},\quad z_{i2}=e^{-i(\alpha/2)}e^{i(\phi/2)}\sin\frac{\theta}{2}. \tag{14}$$

It is natural to introduce the isospin vector $\vec{I}$

$$\vec{I}=z_\alpha^*\vec{\tau}_{\alpha\beta}z_\beta=(\sin\theta\cos\phi,\sin\theta\sin\phi,\cos\theta). \tag{15}$$

Furthermore, it is easy to check that

$$g_i\tau_3 g_i^\dagger=\vec{\tau}\cdot\vec{I}. \tag{16}$$

Thus $\vec{I}$ has the meaning of the local quantization axis parametrized by the polar coordinates θ and ϕ. The angle α in z_i and g_i is redundant and can be absorbed into the phase of b_i in Eq. (12). Using Eq. (12) we can write Eqs. (5) and (6) as

$$Z=\int Dg\ Db\ Db^\dagger D\psi\ D\psi^\dagger D\vec{a}_0 DU\ \exp\left(-\int_0^\beta L'\right), \tag{17}$$

where

$$L' = \frac{\tilde{J}}{2}\sum_{\langle ij\rangle} \mathrm{Tr}(U_{ij}^{\dagger}U_{ij}) + \frac{1}{2}\sum_{i,j,\alpha} \psi_{\alpha i}^{\dagger}[(\partial_\tau + \vec{a}_0\cdot\vec{\tau})\delta_{ij} + \tilde{J}U_{ij}]\psi_{\alpha j}$$
$$+ \sum_{i,j} b_i^{*}\Big(\partial_\tau - \mu + \frac{1}{2}\mathrm{Tr}\{\tau_3[g_i^{\dagger}\vec{a}_0\cdot\vec{\tau}g_i - (\partial_\tau g_i^{\dagger})g_i]\}\delta_{ij}$$
$$+ \frac{\tilde{t}}{2}\mathrm{Tr}[(1+\tau_3)g_i^{\dagger}U_{ij}g_j]\Big) b_j . \tag{18}$$

We see that the path integral of the SU(2) theory is very similar to that of the U(1) theory. Here note that the first line of Eq. (18) is invariant against the local gauge transformation (11). To see this we transform of the integral variables $\psi_{\alpha i} = g_i^{\dagger}\tilde{\psi}_{\alpha i}$, $g_i^{\dagger}U_{ij}g_j = \tilde{U}_{ij}$, and $g_i^{\dagger}\vec{a}_0\cdot\vec{\tau}g_i - (\partial_\tau g_i^{\dagger})g_i = \tilde{\vec{a}}_0\cdot\vec{\tau}$. Then Eqs. (17) and (18) become

$$Z = \int Dg\ Db\ Db^{\dagger}D\tilde{\psi}\ D\tilde{\psi}^{\dagger}D\tilde{\vec{a}}_0 D\tilde{U}\ \exp\Big(-\int_0^{\beta}\tilde{L}'\Big) \tag{19}$$

and

$$\tilde{L}' = \frac{\tilde{J}}{2}\sum_{\langle ij\rangle}\mathrm{Tr}[\tilde{U}_{ij}^{\dagger}\tilde{U}_{ij}]$$
$$+ \frac{1}{2}\sum_{i,j,\alpha}\tilde{\psi}_{i\alpha}^{\dagger}\Big[\Big(\partial_\tau + \sum_{a=1}^{3}\tilde{a}_0^{a}\tau_a\Big)\delta_{ij} + \tilde{J}\tilde{U}_{ij}\Big]\tilde{\psi}_{j\alpha}$$
$$+ \sum_i b_i^{\dagger}(\partial_\tau - \mu + \tilde{a}_0^{3})b_i - \tilde{t}\sum_{i,j}\chi_{ij}b_j^{\dagger}b_i . \tag{20}$$

Note that $\tilde{L}'$ no longer depends on g so that the g integral can be dropped. If we drop the $a_0^{1,2}$ integral, Eqs. (19) and (20) have the same form as the U(1) formulation with an exception that there $\tilde{t}$ is replaced by $t = 2\tilde{t}$. It is not our purpose to derive the exact equivalence between the U(1) and SU(2) path integrals, but rather we want to point out how low-lying fluctuations in the SU(2) formulation may be reproduced in the U(1) picture.

The U(1) mean-field theory corresponds to fixing g to be unity (so that $\vec{I} = \hat{z}$) and finding U_{ij}^{0} and $\vec{a}_0^{(0)}$, which minimizes the action after summing over ψ and b. In the underdoped region, it was found that $U_{ij}^{(0)}$ corresponds to d-wave pairing of fermions. Thus the SU(2) symmetry at half filling is broken by the boson term for finite x. At the same time, it is clear that for $x \ll 1$, there is a host of U(1) mean-field states $U_{ij} = g_i^{\dagger}U_{ij}^{(0)}g_j$ that are close in energy to the d-wave state. Since these states are degenerate at $x = 0$, we may expect an energy cost of order xJ per hole or x^2J per unit cell. An example of special interest is the staggered flux phase that has a Dirac spectrum $E_k = \sqrt{\xi_k^2 + \Delta_k^2}$ at $(\pi/2, \pi/2)$. Since the density of states of the Dirac spectrum is linear in energy, the energy cost is $\sim \mu_F^3/\Delta J$ for a given fermion chemical potential. To satisfy the fermion number constraint, $\mu_F \approx \sqrt{x\Delta J}$ so that in this case the energy cost is expected to be $\sqrt{\Delta J}\ x^{3/2}$ per unit cell. At finite temperatures, we expect that these low-energy configurations should be included in the partition function sum. This additional degree of freedom is just represented by the functional integral over g in Eq. (17) and this is the motivation for adopting the SU(2) formulation.

In Ref. 24 a mean-field theory was introduced for the SU(2) action (5) and (6). The mean field is a saddle point of the action with respect to U_{ij} and $\vec{a}_0$, after integrating over $\psi, \psi^{\dagger}$ and h, $h^{\dagger}$, which is possible because the action is quadratic in these variables. We find that the mean-field phase diagram is only slightly modified from the U(1) case and consists of six different phases. (i) In the staggered flux (s-flux) phase

$$U_{i,i+\hat{x}} = -\tau^3\chi - i(-)^{i_x+i_y}\Delta,$$
$$U_{i,i+\hat{y}} = -\tau^3\chi + i(-)^{i_x+i_y}\Delta, \tag{21}$$

and $a_{0i}^{l} = 0$. In the U(1) slave-boson theory, the staggered flux phase breaks translational symmetry. Here the breaking of translational invariance is a gauge artifact. In fact, a site-dependent SU(2) transformation $W_i = \exp[i(-1)^{i_x+i_y}(\pi/4)\tau_1]$ maps the s-flux phase to the d-wave pairing phase of the fermions: $U_{i,i+\hat{x},\hat{y}} = -\chi\tau_3 \pm \Delta\tau_1$, which is explicitly translationally invariant. In the s-flux phase the fermion and boson dispersions are given by $\pm E_f$ and $\pm E_b$, where $E_f = \sqrt{(\epsilon_f - a_0^3)^2 + \eta_f^2}$, $\epsilon_f = -2\tilde{J}(\cos k_x + \cos k_y)\chi$, $\eta_f = -2\tilde{J}(\cos k_x - \cos k_y)\Delta$, with a similar result for E_b with $\tilde{J}$ replaced by $\tilde{t}$. Since $ia_0^3 = 0$ we have $\langle f_{\alpha i}^{\dagger}f_{\alpha i}\rangle = 1$ and $\langle b_1^{\dagger}b_1\rangle = \langle b_2^{\dagger}b_2\rangle = x/2$. (ii) The π-flux phase is the same as the s-flux phase, except here $\chi = \Delta$. (iii) The uniform RVB (URVB) phase is described by Eq. (21) with $a_{0i}^{l} = \Delta = 0$. (iv) A localized spin phase has $U_{ij} = 0$ and $a_{0i}^{l} = 0$, where the fermions cannot hop. (v) The d-wave superconducting (SC) phase is described by $U_{i,i+\hat{x},\hat{y}} = -\chi\tau_3 \pm \Delta\tau_1$ and $a_0^3 \neq 0$, $a_0^{1,2} = 0$, $\langle b_1\rangle \neq 0$, and $\langle b_2\rangle = 0$. (vi) The Fermi-liquid (FL) phase is similar to the SC phase, except that there is no fermion pairing ($\Delta = 0$).

The connection with the U(1) mean-field theory is now clear by using Eq. (18). The SU(2) mean-field consists of fixing $U_{ij} = U_{ij}^{(0)}$ and $\vec{a}_0 = \vec{a}_0^{(0)}$. For each $\{g_i\}$ the integral over $\psi, \psi^{\dagger}$, $b, b^{\dagger}$ gives the free energy of a U(1) mean-field theory with

$$U_{ij}(g) = g_i^{\dagger}U_{ij}^{(0)}g_j \tag{22}$$

and

$$\vec{a}_0\cdot\vec{\tau} = g_i^{\dagger}a_0^{(0)}\cdot\vec{\tau}g_i + g_i^{\dagger}\partial_\tau g_i . \tag{23}$$

Upon integration over $\{g_i\}$, we see that the SU(2) mean-field theory includes the U(1) mean-field state $\{U_{ij}^{(0)}, \vec{a}_0^{(0)}\}$ and all the configurations $\{U_{ij}, \vec{a}_0\}$ connected to it by SU(2) rotations. Thus, for $x \ll 1$ all the low-energy excitations are included in the partition sum. This is the reason why we believe the SU(2) mean-field theory is a better starting point for underdoped cuprates.

We note that with the exception of the superconducting and Fermi liquid phases, $\vec{a}_0^{(0)} = 0$ in the SU(2) mean-field solution. This means that $\langle f_{\alpha i}^{\dagger}f_{\alpha i}\rangle = 1$ and the constraint (10) is satisfied by $\langle b_1^{\dagger}b_1\rangle - \langle b_2^{\dagger}b_2\rangle = 0$. Unlike the U(1) case, the density of fermions is not necessarily $1 - x$. It is this feature

that allows the staggered-flux and d-wave states to be gauge equivalent descriptions in the s-flux phase, for instance. One consequence is that the node in the gap function of the fermion excitation is pinned at $(\pi/2,\pi/2)$. In Ref. 24 it was found that by including an attraction between the boson and fermion due to the exchange of a_0 fluctuations, Fermi-surfacelike features can be recovered in the physical electron spectral weight that is shifted away from $(\pi/2,\pi/2)$.

A similar situation appears in the URVB phase. The fermion Fermi surface encloses area 1 and one must go beyond mean-field theory to produce electron Fermi-surfacelike features that obey the Luttinger theorem. The problem is even more serious in the FL phase. Even though a_0^3 is now not equal to zero, the fermion Fermi surface area approaches $1-x$ only very slowly with increasing x and decreasing temperature. The FL state exists only for $x \geqslant J/t$, so the motivations behind the SU(2) mean-field theory are no longer applicable. Nevertheless, this observation means that the SU(2) mean-field theory does not evolve towards the U(1) mean-field theory in a way that is acceptable.

We believe the origin of these difficulties lies in fixing $\vec{a}_0^{(0)}$ as a mean-field parameter from the beginning. For $\vec{a}_0^{(0)}=0$, the constraint is satisfied on the average by $\langle h^\dagger \vec{\tau} h\rangle = 0$. For example, this implies $\langle b_{1i}^\dagger b_{2i}\rangle = 0$. Using Eqs. (13) and (15), this suggests that the isospin vector $\vec{I}$ is randomized so that $\langle \vec{I}_i\rangle = 0$. On the other hand, as we approach the superconducting phase boundary T_c from above or the Fermi-liquid boundary from the URVB side, the boson field h_i becomes phase coherent and we expect that it should be slowly varying in space and time. In these regions, the short-range correlation of the boson field is not captured by the SU(2) mean-field theory. This motivates us to formulate an alternative effective theory for the SU(2) partition function, which we shall refer to as the σ-model description.

Our strategy is to pick a mean-field configuration $U_{ij}^{(0)}$ and consider a slowly varying configuration h_i in Eq. (6) or, equivalently, a slowly varying g_i and b in Eq. (18). For each configuration, $\vec{a}_0$ is solved to satisfy the constraint locally, after performing the integral over $\psi,\psi^\dagger$. Thus, in principle $\vec{a}_0$ is a functional of $\{\vec{h}_i\}$. Our final goal is to produce an effective Lagrangian for $\{\vec{h}_i\}$ that will take the form of some nonlinear σ model to describe the low-energy physics of the problem. This is the opposite limit to the SU(2) mean-field theory: The assumption of a uniform $\vec{a}_0$ is valid when the h_i configurations are rapidly varying on the scale of the fermion correlation length, which is of order $\xi_0=\epsilon_F/\Delta$ in the s-flux phase. This picture is valid at high temperatures, whereas the σ-model approach is expected to be applicable near the superconducting transition and the crossover to the Fermi-liquid state. The truth most likely lies in between the two extreme limits in most parts of the phase diagram and it will be of interest to explore the consequences of both limits.

It is clear that any $\tilde{U}_{ij}^{(0)}$ related to $U_{ij}^{(0)}$ by a SU(2) gauge transformation will give an equivalent description. Thus we can start with any U(1) mean-field configuration. In principle, we should optimize the parameters χ and Δ at the end of the calculation, but in practice we expect these parameters to be not so different from that given by the U(1) mean-field theory. We also find that a judicial choice of $U_{ij}^{(0)}$ that exhibits the symmetry of a given phase yields a σ model that exhibits the proper symmetry. As a first example we discuss the URVB state.

III. σ MODEL OF THE FERMI LIQUID AND THE URVB PHASES

In U(1) mean-field theory the matrix $U_{ij}^{(0)}$ in the URVB state is given by $U_{ij}^{(0)}=\begin{pmatrix} -\chi_{ij}^* & 0 \\ 0 & \chi_{ij}\end{pmatrix}$. Here we make the choice $\chi_{ij}=i\chi_0$, so that $U_{ij}^{(0)}=i\chi_0 I$ is proportional to the identity element. Thus $U_{ij}^{(0)}$ itself is invariant under a global SU(2) transformation.

For $a_0^1=a_0^2=0$ the bosons b_1 and b_2 are diagonalized by the energy dispersion

$$E_b^{1,2}=-2t\chi_0(\sin k_x+\sin k_y)\pm a_0^3-\mu. \tag{24}$$

In the Fermi-liquid phase, the boson condenses to the bottom of the band, located for this choice of gauge at $Q_0=(\pi/2,\pi/2)$.

As explained in Ref. 24 the SU(2) mean-field theory solution for the Fermi liquid is given by $a_0^3<0$ and b_1 contains a Bose-condensed part so that $\langle b_1\rangle = b_0 e^{i\vec{Q}_i\cdot\vec{r}}$. Note that at finite T, thermal excitations make $\langle b_2^\dagger b_2\rangle \neq 0$. From Eqs. (8) and (10) we see that the fermion density

$$\left\langle \sum_\alpha f_{i\alpha}^\dagger f_{i\alpha}\right\rangle = 1-x+2\langle b_2^\dagger b_2\rangle \tag{25}$$

is not equal to $1-x$, so that Luttinger theorem is not obeyed. As discussed in the Introduction, this motivates us to try the σ-model approach, where we write

$$h_i=\tilde{h}_i e^{i\vec{Q}_0\cdot\vec{r}} \tag{26}$$

and look for $\tilde{h}_i$ that is slowly varying in space and τ. We can further parametrize $\tilde{h}_i=g_i\binom{b}{0}$. Locally we can consider $g_i=g_0$ as constant. By introducing $\tilde{\psi}=g_i^\dagger\psi$ we see that L' in Eq. (18) takes the U(1) form

$$\begin{aligned} L' = &\frac{1}{2}\sum_{i,j,\alpha}\tilde{\psi}_{i\alpha}^\dagger[(\partial_\tau+\vec{a}_0'\cdot\vec{\tau})\delta_{ij}+\tilde{J}U_{ij}^{(0)}]\tilde{\psi}_{i\alpha}+\sum_{i,j} b_i^* \\ &\times\Bigg(\partial_\tau-\mu+\frac{1}{2}\mathrm{Tr}[\tau_3(\vec{a}_0'\cdot\vec{\tau})]\delta_{ij} \\ &+\frac{\tilde{t}}{2}\mathrm{Tr}[(1+\tau_3)U_{ij}^{(0)}]\Bigg)b_j, \end{aligned} \tag{27}$$

where

$$\vec{a}_0'\cdot\vec{\tau}=g_i^\dagger\vec{a}_0\cdot\vec{\tau}g_i-(\partial_\tau g^\dagger)g. \tag{28}$$

The local U(1) mean-field solution of Eq. (26) is given by $\vec{a}_0'=a_{00}\hat{z}$ and a_{00} is the fermion chemical potential chosen in a way that ensures that the $\tilde{\psi}$ fermion density is $1-x$. From Eqs. (26) and (16) we find that

$$\vec{a}_{0i}=a_{00}\vec{I}(g_i). \tag{29}$$

The physical electron Green function in the SU(2) theory

$$G(\vec{r},\tau) = -\langle T_\tau[c_1(\vec{r},\tau)c_1^\dagger(\vec{0},0)]\rangle$$
$$= -\frac{1}{2}\langle T_\tau[h^\dagger(\vec{r},\tau)\psi_1(\vec{r},\tau)\psi_1^\dagger(\vec{0},0)h(\vec{0},0)]\rangle. \tag{30}$$

Assuming b is Bose condensed, we have, within the mean-field theory,

$$G(r,\tau) = -\frac{1}{2}b_0^2\langle T_\tau[\tilde{f}_1(\vec{r},\tau)\tilde{f}_1^\dagger(0,0)]\rangle + (\text{incoherent part}). \tag{31}$$

The fermion part $\tilde{\psi}_\alpha$ and therefore the physical electron Fermi surface now satisfy the Luttinger theorem in this slowly varying approximation.

We would like to remark that the electron Green function in the U(1) theory has the form

$$G(\vec{r},\tau) = -\langle T_\tau[c_\uparrow(\vec{r},\tau)c_\uparrow^\dagger(\vec{0},0)]\rangle$$
$$= -\langle T_\tau[b^\dagger(\vec{r},\tau)f_\uparrow(\vec{r},\tau)f_\uparrow^\dagger(\vec{0},0)b(\vec{0},0)]\rangle. \tag{32}$$

The U(1) mean-field Green function is

$$G(r,\tau) = -b_0^2\langle T_\tau[f_\uparrow(\vec{r},\tau)f_\uparrow^\dagger(0,0)]\rangle + (\text{incoherent part}) \tag{33}$$

after the boson condensation. Although the coherent part has the same dispersion relation, the quasiparticle weight in the U(1) mean-field Green function is twice the quasiparticle weight in the SU(2) mean-field Green function.

We next derive an explicit expression for the σ-model Lagrangian by expanding in a_0 and integrating out the fermion. This is a systematic procedure for small x. Starting from Eq. (5), the fermion integration yields a contribution $-\mathrm{Tr}\,\ln(\partial_\tau + \tilde{J}U_{ij}^{(0)} - i\vec{a}_0\cdot\vec{\tau})$. An expansion in $\vec{a}_0$ to quadratic order yields the term

$$\mathcal{L}'_F = \sum_{q,\omega_n}\frac{1}{2}a_0^\alpha(q,\omega_n)a_0^{*\beta}(q,\omega_n)\pi_{00}^{\alpha\beta}(q,\omega_n), \tag{34}$$

where

$$\pi_{00}^{\alpha\beta}(q,\omega_n) = \int_0^\beta d\tau\, e^{i\omega_n\tau}\sum_i e^{-i\vec{q}\cdot(\vec{r}_i-\vec{r}_j)}$$
$$\times\langle\psi_i^\dagger\tau_\alpha\psi_i(\tau)\psi_j^\dagger\tau_\beta\psi_j(0)\rangle. \tag{35}$$

For the URVB state, $\pi_{00}^{\alpha\beta} = \pi_{00}^{(0)}\delta_{\alpha\beta}$, where $\pi_{00}^{(0)}$ may be expanded for small q and $|\omega_n| < q$ as

$$\pi_{00}^{(0)}(q,\omega) = \pi_0 + C_1'J^{-1}q^2 + C_2'J^{-2}\frac{|\omega_n|}{q}. \tag{36}$$

The coefficient $\pi_0 = -C_0'J^{-1}$, and C_0', C_1', and C_2' are constants of order unity. The leading term gives a contribution $-C_0'J|a_0|^2$. The negative sign is a reminder that the mean field a_0 is a saddle point with the stable direction along the imaginary axis. We shall see that this negative sign yields correctly a repulsive interaction between the bosons.

We expand in $\tilde{h}$ about the bottom of the boson bands and the effective Lagrangian takes the form

$$\mathcal{L}_{eff} = \tilde{h}^\dagger\partial_\tau\tilde{h} + \frac{1}{2m_b}|\partial_i\tilde{h}|^2 - \mu\tilde{h}^\dagger\tilde{h}$$
$$+ D_1 m_b^{-1}(\tilde{h}^\dagger\tilde{h})^2 + |b|^2\vec{a}_0(\vec{r},\tau)\cdot\vec{I}(\vec{r},\tau)$$
$$+ \frac{1}{2}\sum_{q,\omega_n}|a_0(q,\omega_n)|^2\pi_{00}^{(0)}(q,\omega_n). \tag{37}$$

The D_1 term is used to model the repulsion between bosons and D_1 is of order unity for infinite on-site repulsion. We have rewritten the coupling between $\tilde{h}$ and $\vec{a}_0$ using Eqs. (16) and (12). Since Eq. (37) is quadratic in a_0, it can be eliminated, yielding a fermion contribution to the Lagrangian

$$\mathcal{L}''_F = -\frac{1}{2}\sum_{q,\omega_n}\frac{|b|^4\vec{I}^*(q,\omega_n)\cdot\vec{I}(q,\omega_n)}{\pi_{00}^{(0)}(q,\omega_n)}$$
$$\approx -\frac{1}{2}|b|^4\sum_{q,\omega_n}\vec{I}^*(q,\omega_n)\cdot\vec{I}(q,\omega_n)$$
$$\times\left(-C_0J + C_1Jq^2 + C_2\frac{|\omega_n|}{q}\right). \tag{38}$$

Using $\vec{I}\cdot\vec{I}\equiv 1$, the first term is $\frac{1}{2}C_0J|b|^4$ and it modifies the D_1 term in Eq. (37) to $D_1' = D_1 + C_0J$. For $J < t$, this is a small correction. To obtain a description in terms of the z fields $z = (z_1, z_2)$, where z_1, z_2 are defined in Eq. (13), we write $\tilde{h} = (b_0 + \delta b)z$ and integrate out the δb field. We find

$$\mathcal{L}_{eff} = \frac{2}{3}\frac{m_b}{D_1'}|z^\dagger\partial_\tau z|^2 + |b_0|^2 z^\dagger\partial_\tau z + \frac{x}{2m_b}|\partial_i z|^2 + \mathcal{L}_F, \tag{39}$$

$$\mathcal{L}_F = \frac{1}{2}x^2J\sum_{q,\omega_n}\vec{I}^*(q,\omega_n)\cdot\vec{I}(q,\omega_n)\left(C_1q^2 + C_2\frac{|\omega_n|}{q}\right). \tag{40}$$

We have approximated b^2 by x and b_0 is a constant of order $\sqrt{x}$ at low temperature. The first term in Eq. (40) is a ferromagnetic Heisenberg interaction between the isospins. Using the usual CP^1 representation, it can be written as

$$\frac{C_1}{2}x^2J|(\partial_i - i\tilde{A}_i)z|^2, \tag{41}$$

where

$$\tilde{A}_i = \frac{i}{2}[z^\dagger\partial_i z - (\partial_i z^\dagger)z]. \tag{42}$$

Note that whereas the boson part in Eq. (39) has the full O(4) symmetry, the fermion part has only O(3) symmetry because it is independent of the overall phase α. The second term in Eq. (40) describes dissipation due to particle-hole excitations of the Fermi sea. Note that the fermion contribution is proportional to x^2J, which is smaller than the boson contribution, which is proportional to xt even in the overdoped region ($xt \geq J$). For example, if $T > x^2J$ we can ignore the

fermion term and if we further make the classical approximation, we conclude that at high temperatures the system is described by the classical O(4) model. There is no phase transition but instead there is a crossover temperature of order xt below which the phase coherence length grows exponentially. This is opposed to the U(1) mean-field theory where there is a Kosterlitz-Thouless transition. Of course this transition is destroyed when gauge fluctuations are taken into account.[29] However, in our case vortex excitations are destroyed by SU(2) fluctuations and we can expect a suppression of the development of phase coherence in the SU(2) formulation due to the addition of low-lying degrees of freedom. It is interesting to ask what the nature of these low-energy excitations is. In the effective Lagrangian (39), the degeneracy for constant z is a gauge symmetry: Any constant z is related by a global gauge transformation to the U(1) URVB state. When z is slowly varying, we can use Eq. (22) to see that in the U(1) representation, $U_{ij}=i\chi_0 g_i g_j^\dagger$ is generated, which in general contains pairing amplitudes Δ_{ij} as well as modifications of the hopping term χ_{ij} which affects both the boson and fermion energy. This is in contrast to the U(1) formulation, where only the phase fluctuation of χ_{ij} is included. Thus we may view the SU(2) formulation as a way to discover low-lying excitations that were not so obvious in the U(1) picture. To complete the discussion of the low-lying excitations we need to introduce gauge fields to the effective Lagrangian. This will be done in a later section.

IV. σ MODEL OF THE SUPERCONDUCTING AND THE STAGGERED-FLUX PHASES

We repeat the procedure in the preceding section for the staggered-flux phase by choosing an appropriate $U_{ij}^{(0)}$ matrix. Once again any $U_{ij}^{(0)}$ that are related by gauge transformations will give the same result, but it will be convenient to use a $U_{ij}^{(0)}$ that exhibits the symmetry of the state. We have noted before that in the SU(2) mean-field theory, the s-flux state breaks the SU(2) symmetry down to U(1). This motivates us to choose the following $U_{ij}^{(0)}$ to describe the s-flux phase.

We choose the following ansatz to describe the s-flux phase:

$$U_{i,i+\hat{x}}^{(0)}=-i\chi-(-1)^i\tau^3\Delta, \quad U_{i,i+\hat{y}}^{(0)}=-i\chi+(-1)^i\tau^3\Delta, \tag{43}$$

and

$$a_0^l(i)=a_0^l+(-1)^i\tilde{a}_0. \tag{44}$$

Note that $U_{ij}^{(0)}$ is invariant under global τ_3 rotations. In the momentum space $\psi_i=\Sigma_i e^{-i\vec{k}\cdot\vec{i}}\psi_k$, we have

$$H_{mean}^f=\tilde{J}\sum_k{}'(\psi_k^\dagger,\psi_{k+Q}^\dagger) \times\begin{pmatrix} V_k+a_0^l\tau^l & W_{k+Q}+\tilde{a}_0^l\tau^l \\ W_k+\tilde{a}_0^l\tau^l & V_{k+Q}+a_0^l\tau^l \end{pmatrix}\begin{pmatrix} \psi_k \\ \psi_{k+Q} \end{pmatrix},$$

$$H_{mean}^b=\tilde{t}\sum_k{}'(h_k^\dagger,h_{k+Q}^\dagger)\begin{pmatrix} V_k+a_0^l\tau^l & W_{k+Q}+\tilde{a}_0^l\tau^l \\ W_k+\tilde{a}_0^l\tau^l & V_{k+Q}+a_0^l\tau^l \end{pmatrix} \times\begin{pmatrix} h_k \\ h_{k+Q} \end{pmatrix}, \tag{45}$$

where

$$V_k=-2\chi(\sin k_x+\sin k_y)=-2\chi\alpha_k,$$
$$W_k=-2i\tau^3\Delta(\sin k_x-\sin k_y)=-2i\tau^3\Delta\gamma_k, \tag{46}$$

and Σ_k' represents summation over half of the Brillouin zone.

To study the boson-condensed phase at low temperatures, let us first assume that $\tilde{a}_0^l=0$. In this case the boson band bottom is at $k=(\pi/2,\pi/2)$ if a_0^l is not too large. Thus the condensed boson has the form

$$\begin{pmatrix} b_1(i) \\ b_2(i) \end{pmatrix}=\begin{pmatrix} b_1 \\ b_2 \end{pmatrix}e^{-i(i_x+i_y)\pi/2}. \tag{47}$$

For such a boson condensation the boson free energy is an even function of $\tilde{a}_0^l$. We also note that

$$M(k_x,k_y,a_0^l,\tilde{a}_0^l)=\begin{pmatrix} V_k+a_0^l\tau^l & W_{k+Q}+\tilde{a}_0^l\tau^l \\ W_k+\tilde{a}_0^l\tau^l & V_{k+Q}+a_0^l\tau^l \end{pmatrix} =\begin{pmatrix} -2\chi\alpha_k+a_0^l\tau^l & 2i\Delta\tau^3\gamma_k+\tilde{a}_0^l\tau^l \\ -2i\Delta\tau^3\gamma_k+\tilde{a}_0^l\tau^l & 2\chi\alpha_k+a_0^l\tau^l \end{pmatrix} \tag{48}$$

satisfies

$$M(k_x,k_y,a_0^l,\tilde{a}_0^l)=\begin{pmatrix} 1 & & & \\ & 1 & & \\ & & -1 & \\ & & & -1 \end{pmatrix} \times M(k_y,k_x,a_0^l,-\tilde{a}_0^l) \times\begin{pmatrix} 1 & & & \\ & 1 & & \\ & & -1 & \\ & & & -1 \end{pmatrix}. \tag{49}$$

Thus the fermion free energy is also an even function of $\tilde{a}_0^l$. Therefore, $\tilde{a}_0^l=0$ is a self-consistent solution.

We would like to remark that U_{ij} in Eq. (43) does not contain any fermion pairing. However, the boson condensate induces nonzero a_0^l. A nonzero $a_0^{1,2}$ induces a pairing condensate of the fermions. But when $a_0^{1,2}=0$ there is no pairing and the fermions are in a normal Fermi-liquid state.

Now we are ready to discuss some basic physical properties of our ansatz for different orientation of the condensate (b_1,b_2). Without lose of the generality, we may assume b_1/b_2 to be real. In this case $a_0^2=0$. We see that when $b_1=b_2$ (in this case $a_0^3=0$) the ansatz describes a translation and rotation invariant state. This state is equivalent to the

usual d-wave paired state in the U(1) mean-field theory after an SU(2) gauge transformation. It describes a d-wave superconducting state (with a finite chemical potential) of the t-J model. When $b_1 \neq b_2$ and $b_1 b_2 \neq 0$, we have $a_0^3 \neq 0$ and $a_0^1 \neq 0$. There is a pairing condensate in the fermions. The ansatz describes a superconducting state of the t-J model that also breaks the translation symmetry. The quasiparticle excitations have finite gap except at four isolated points near $(\pm\pi/2, \pm\pi/2)$. When $b_1 \neq 0$ and $b_2 = 0$, we have $a_0^3 \neq 0$ and $a_0^{1,2} = 0$. There is no pairing condensate in the fermions. The ansatz, despite the boson condensate, does not correspond to a superconducting state. It instead describes a Fermi liquid with broken translation symmetry and small pocketlike Fermi surfaces. This result is obtained through a later calculation of electromagnetic response.

At high enough temperatures, the thermal fluctuations make $\langle b_1 \rangle = \langle b_2 \rangle = \langle a_0^l \rangle = 0$. In this case the ansatz describes a translation and rotation invariant metallic state, which is just the s-flux phase studied in Ref. 24

In order to derive a σ model for the $\tilde{h}$ field, we integrate out the fermions as before. The difference now is that $\pi_{00}^{\alpha\beta} = \pi_{00}^{\alpha} \delta_{\alpha\beta}$, where $\pi_{00}^x = \pi_{00}^y \neq \pi_{00}^z$. We find that $\pi_{00}^x(0) \approx C_1' J$, whereas $\pi_{00}^z(0) = 0$ for $\vec{a}_0 = 0$. This is because π^z is the density-density response function and $\pi^z(0)$ is the compressibility of the fermion that vanishes due to the vanishing density of states in the middle of the band. For finite a_0^3 we find that $\pi_{00}^z(0) = C_2' a_0^3$. Now we can eliminate $\vec{a}_0$ to extremize the action. The problem retains rotational symmetry in the x-y plane, but is anisotropic in the z direction. For example, for $\vec{I}$ in the x-y plane, we have $a_0^3 = 0$ and the energy of the mean-field state is

$$E_{\mathrm{MF}} = -4t\chi x + \frac{J}{2C_1'} x^2. \tag{50}$$

On the other hand, for $\vec{I} = \hat{z}$, we have $a_0^1 = a_0^2 = 0$. Eliminating a_0^3 we find the mean-field energy to be

$$E_{\mathrm{MF}} = -4t\chi x + \frac{2J}{3\sqrt{C_2'}} x^{3/2}. \tag{51}$$

This result indicates that the boson condensate tends to stay in the manifold that satisfies $|b_1| = |b_2|$, i.e., $I_z = 0$. As pointed out earlier, this state is equivalent to the d-wave pairing state as opposed to the state $\vec{I} = \hat{z}$, which corresponds to the staggered-flux state with finite chemical potential.

We can follow the procedure of Sec. III to derive an effective Lagrangian for the z field. The important difference is the appearance of the anisotropy energy. Ignoring the gradient terms from the fermion contribution, we can write down the effective Lagrangian

$$\mathcal{L}_{\mathrm{eff}} = \frac{2}{3}\frac{m_b}{D_1}|z^\dagger \partial_\tau z|^2 + x z^\dagger \partial_\tau z + \frac{x}{2m_b}|\partial_i z|^2 + \frac{x^2 J'}{2C_1} 4|z_1 z_2|^2 + \frac{x^2 J'}{2C_3}(|z_1|^2 - |z_2|^2)^2. \tag{52}$$

The last two terms are introduced phenomenologically to model the breaking of the O(3) symmetry down to x-y symmetry when $C_1 \neq C_3$. This is adequate for $\vec{I}$ near the x-y plane but, strictly speaking, needs further modification near the north and south poles, due to the singular behavior of the energy cost given by Eq. (51).

To gain some understanding of the phases of the nonlinear σ model, let us consider the classical limit where the τ dependence of z is neglected. If (z_1, z_2) is restricted to the manifold of minimum energy, i.e., $\vec{I}$ is in the x-y plane, the model is equivalent to two x-y models, with the Kosterlitz-Thouless transition at $T_{\mathrm{KT}} \approx (1/4m_b)\pi x$. This temperature scale will be suppressed by fluctuations of $\vec{I}$ out of the x-y plane because the energy cost per unit area is only $x^2 J$. However, we need to introduce gauge fields to Eq. (52) before the low-lying excitations can be fully discussed.

V. THE ELECTRON SPECTRAL FUNCTION IN THE σ-MODEL DESCRIPTION

In this section we compute the physical electron Green function $G(\vec{r}, \tau)$ assuming that we are in the disordered phase of the σ-model description. We have within the mean-field theory

$$G(\vec{r}, \tau) = -\frac{1}{2}\langle T_\tau h^\dagger \psi(\vec{r}, \tau) \psi^\dagger(0,0) h \rangle \tag{53}$$

$$\approx G_B(\vec{r}, \tau) G_F(\vec{r}, \tau), \tag{54}$$

where

$$G_B(\vec{r}, \tau) = \langle T_\tau [h^\dagger(\vec{r}, \tau) h(0,0)] \rangle, G_F(\vec{r}, \tau) = -\langle T_\tau [\tilde{\psi}(\vec{r}, \tau) \tilde{\psi}^\dagger(0,0)] \rangle. \tag{55}$$

The boson Green function contains two parts. Note that at temperature T most bosons are in states that have energies of order T from the bottom of the boson band. Thus at high energies the boson Green function is given by the single-boson Green function G_B^s as if no other bosons are present. The imaginary part of this part of boson Green function extends the whole bandwidth of the boson band. At low energies (of order T), the boson Green function is determined by those nearly condensed bosons at low energies. Thus we may assume that bosons do condense and the second part of the boson Green function can be approximated by $\mathrm{const} \times e^{i Q_b \vec{r}}$, where Q_b is the momentum of the bottom of the boson band. From the above discussion we see that the mean-field electron Green function has the form

$$G_e^{(0)} = \mathrm{const} \times e^{i Q_b \vec{r}} G_F + G_{in}^{(0)}. \tag{56}$$

The second term comes from the convolution of $G_B^{(s)}$ and G_F and is the incoherent part of the Green function. The first term is the coherent part since its imaginary part is given by discrete δ functions. (Note those discrete δ-function peaks should really have a finite width of order T if the bosons do not really condense as in the s-flux and URVB phases.) It is this coherent part that gives rise to the quasiparticle peaks observed in photoemission experiments. The more exact ex-

pression of $G_e^{(0)}$ is given by Eq. (C1) in Appendix C. At low temperatures the lengthy expression can be simplified as

$$G_e^{(0)}(\omega,k)\simeq\frac{x}{2}\left[\frac{[v^f(k)]^2}{\omega-E_-^f(k)}+\frac{[u^f(k)]^2}{\omega-E_+^f(k)}\right]+G_{in}^{(0)}. \quad (57)$$

The incoherent part satisfies

$$\int_{-\infty}^{+\infty}\frac{d\omega}{\pi}\mathrm{Im}G_{in}^{(0)}=\frac{1}{2}, \quad (58)$$

which can be shown by using Eq. (C1).

In the following we go beyond the mean-field theory and discuss several corrections to the mean-field Green function. As low energies, bosons are nearly condensed. The boson fields (b_1,b_2) [or $g_i(t)$] change slowly in the time direction (within a range of order $1/T$) and in the spatial direction (within a range of order $a\sqrt{t/T}$). Thus locally we may think there is really a boson condensation and calculate the (mean-field) electron Green function in the boson-condensed phase. Since in the different regions the boson fields (b_1,b_2) point to different directions, the total Green function can be obtained by averaging the mean-field Green functions for all the directions. We would like to point out that the fermion Green functions are different for different directions of the boson fields because different local boson fields give rise to different local a_0^l that enforces the constraint.

The above picture of calculating the electron Green function naturally comes from our σ-model treatment of the SU(2) theory. The averaging weights for different directions are determined from the σ model. We now make the crude approximation that we are in the high-temperature phase of the σ model, where all slowly varying configurations z are equally likely.

We have already seen in Sec. III that this procedure yields a Fermi surface that obeys the Luttinger theorem in the Fermi-liquid phase where the bosons are condensed and in the URVB phase where the bosons are nearly condensed. The fluctuations of the boson fields in the URVB phase will give rise to finite broadening of the quasiparticle peaks. We now perform the same procedure in the s-flux phase.

For each uniform configuration $g_i=g$, $\mathrm{Im}G_F(\omega,k)$ in general contains four δ-function peaks as a function of ω. (Note that for general g we have both translation symmetry breaking and fermion pairing.) After averaging over all orientations of g, we get a translation invariant electron Green function. This averaging also gives quasiparticle peaks an intrinsic width and line shape.

Figure 1 presents a numerical calculation of the electron spectral function using the above approximation. We have chosen $\tilde{J}=J/2$ and $\chi=1$ so that the fermion band bottom is at around $-2J$, to be consistent with experiments. We have set $\tilde{t}=t=2J$ so that the incoherent part of the spectral function extends from $-8t=-16J$ to 0, in order to agree with the numerical results. We have also set $\Delta/\chi=0.2$ so that the gap near $(0,\pi)$ is about $0.4J$. Roughly, the spectral function is similar to that of a d-wave paired state with a spin gap around $(0,\pm\pi)$ and $(\pm\pi,0)$ of order $\Delta_{\mathrm{spin}}\sim 0.4J$. However, the line shape and linewidth are quite different. If one plots $\mathrm{Im}G(\omega=0,k)$ one can see that wings toward $(0,\pi)$ and

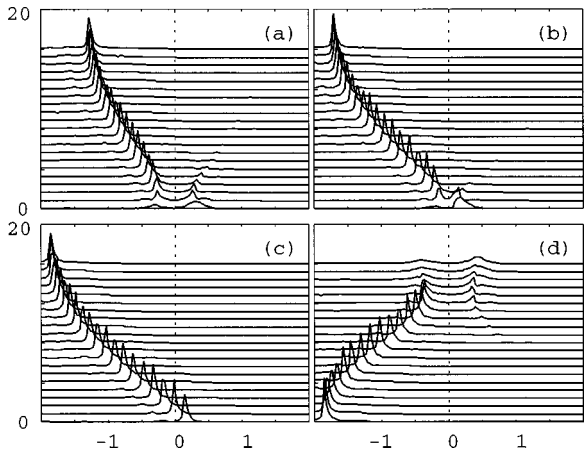

FIG. 1. Electron spectral function. The x axis is the frequency. The curves are for the following values of k, from top down to bottom: (a) $k=(-\pi/4,\pi/4)\rightarrow(\pi/4,3\pi/4)$, (b) $k=(-\pi/8,\pi/8)\rightarrow(3\pi/8,5\pi/8)$, (c) $k=(0,0)\rightarrow(\pi/2,\pi/2)$, and (d) $k=(0,\pi)\rightarrow(0,0)$. We have chosen $J=1$.

$(0,\pi)$ at two sides of the peak [at $(\pi/2-\delta,\pi/2-\delta)$] are enhanced by the averaging. It is because when $g=1$, $\mathrm{Im}G(\omega=0,k)$ has a Fermi pocket around $(\pm\pi/2,\pm\pi/2)$. We see that the averaging over g pushes the d-wave spectrum towards a spectrum that shows a segment of Fermi surface.

In the above calculation of the spectral function, we only include some simple fluctuations (i.e., the uniform fluctuations of boson field). One may wonder how reliable the above result is. In the following we calculate $\mathrm{Im}G_e$ by including some different fluctuations. We find that the spin gaps around $(0,\pm\pi)$ and $(\pm\pi,0)$ are quite robust. However, the low-energy spectral function near $(\pm\pi/2,\pm\pi/2)$ (together with the positions and the shapes of the Fermi segments) are sensitive and are essentially determined by the fluctuations. Although different fluctuations have different effects, they in general stretch Fermi points of the mean-field theory into Fermi segments.

The dominant effect of fluctuations is to bind the bosons and the fermion into an electron. This corresponds to an effective attraction between the bosons and the fermions. One way to include this effect is to use the diagram in Fig. 2 to approximate the electron Green function, which corresponds to an effective short-range interaction of the form

$$-\frac{V}{2}(\psi^\dagger h)(h^\dagger\psi)=-Vc^\dagger c, \quad (59)$$

with $V<0$. We get

$$G_e=\frac{1}{(G_e^{(0)})^{-1}+V}. \quad (60)$$

FIG. 2. Diagram for renormalized electron Green function. The solid (dashed) line is the fermion (boson) propagator.

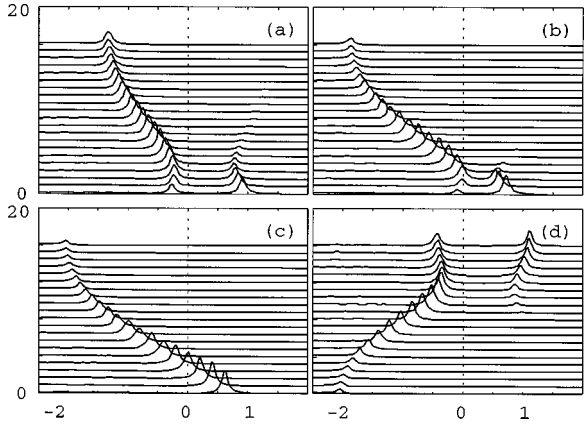

FIG. 3. Electron spectral function. The curves are for the following values of k, from top to bottom: (a) $k=(-\pi/4, \pi/4)\rightarrow(\pi/4,3\pi/4)$, (b) $k=(-\pi/8,\pi/8)\rightarrow(3\pi/8,5\pi/8)$, (c) $k=(0,0)\rightarrow(\pi/2,\pi/2)$, and (d) $k=(0,\pi)\rightarrow(0,0)$. We have chosen $J=1$. The paths of the four momentum scans are shown in Fig. 5.

However, in general, fluctuations induce more complicated interactions. A more careful treatment can be found in Appendix C, where we treat two different kinds of fluctuations. The first one is the fluctuation of a_0, which induces the following interaction between the fermions and the bosons:

$$\psi^\dagger\vec{\tau}\psi\cdot h^\dagger\vec{\tau}h. \tag{61}$$

The second one (whose importance was pointed out by Laughlin[30]) is the fluctuation of $|\chi_{ij}|$, which induces

$$-t(\psi^\dagger h)_j(h^\dagger\psi)_i=-2tc_j^\dagger c_i. \tag{62}$$

This is nothing but the original hopping term. We expect the coefficient t to be reduced due to screening, but in the following we adopt the form

$$V(k)=U+2t(\cos k_x+\cos k_y) \tag{63}$$

for V in Eq. (60). Here the first and the second term comes from the first and the second kind of fluctuations. In Figs. 3 and 4 we plot the electron spectral function calculated from Eq. (60). We have chosen $\tilde{J}=J/2$, $\tilde{t}=t=2J$, $\chi=1$, $\Delta/\chi=0.4$, $x=0.1$, and $T=0.1J$. Here we choose $\Delta/\chi=0.4$, so that the renormalized gap near $(0,\pi)$ is about $0.4J$. The value U is determined from requiring the renormalized electron Green function to satisfies the sum rule

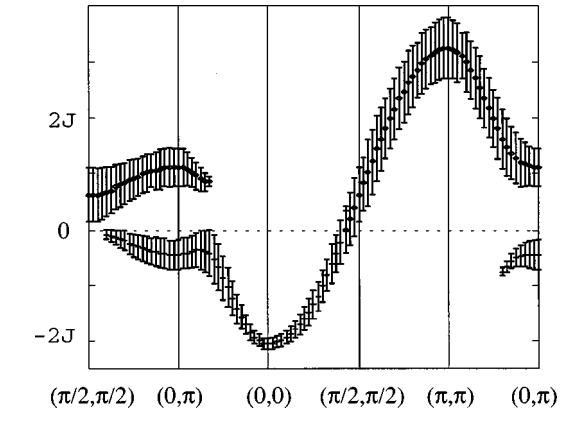

FIG. 4. The points describe the dispersion of the quasiparticle peaks for the s-flux phase in Fig. 3. The vertical bars are proportional to the peak values of $\mathrm{Im}G_U$, which are proportional to the quasiparticle weight.

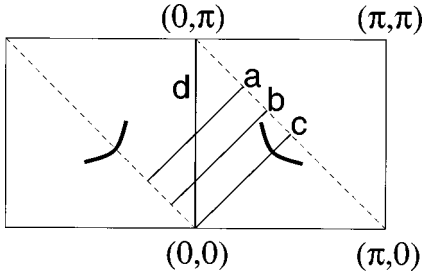

FIG. 5. Solid lines a, b, c, and d are paths of the four momentum scans in Fig. 3. The solid curves are a schematic representation of the Fermi segments where the quasiparticle peak crosses the zero energy.

$$\int_0^\infty\frac{d\omega}{2\pi}\int\frac{d^2k}{(2\pi)^2}\mathrm{Im}G_e=x. \tag{64}$$

Note that the mean-field electron Green function in Eq. (C1) does not satisfy this sum rule

$$\int_0^\infty\frac{d\omega}{2\pi}\int\frac{d^2k}{(2\pi)^2}\mathrm{Im}G_e^{(0)}=x/4. \tag{65}$$

We find that the gap near $(0,\pm\pi)$ and $(\pm\pi,0)$ survives the inclusion of gauge and $|\chi_{ij}|$ fluctuations. However, spectral functions near $(\pm\pi/2,\pm\pi/2)$ are modified. The Fermi point at $(\pi/2,\pi/2)$ for the mean-field electron Green function $G_e^{(0)}$ is stretched into a Fermi segment as shown in Fig. 5. We would like to point out that the electron Green function obtained here does not show any ''shadow band'' at $\omega=0$, i.e., $\mathrm{Im}G_e(0,k)$ does not have any peak outside the $(0,\pi)$-$(\pi,0)$ line as the mirror image of the peaks that appear inside the $(0,\pi)$-$(\pi,0)$ line.

The spectral function obtained here is qualitatively similar but quantitatively different from the one obtained in Ref. 24 through a similar calculation. The only difference is that here we include an additional term $2t(\cos k_x+\cos k_y)$. Without this term the quasiparticle peaks near $(0,0)$ get strongly renormalized and become very strong. The quasiparticle energies near $(0,0)$ get pushed so high that they are nearly degenerate with the energy gap near $(0,\pi)$. Those features obviously disagree with experimental observations. After including the $2t(\cos k_x+\cos k_y)$ term the agreement with experiments improved a lot. Due to a cancellation between the U and $2t(\cos k_x+\cos k_y)$ near $k=(0,0)$, the quasiparticle energies and spectral weights near $(0,0)$ are quite close to the mean-field values and the gap at $(0,\pi)$ now can be quite different from the quasiparticle energy at $(0,0)$.

The incoherent part of the electron spectral function contains two broad peaks, each with a width about $4t$. The incoherent part of the electron spectral function is roughly given by the boson density of states. In the SU(2) theory, the bosons experience the staggered flux, which causes the double-peak structure in the boson density of states and in the incoherent part of the electron spectral function. As we

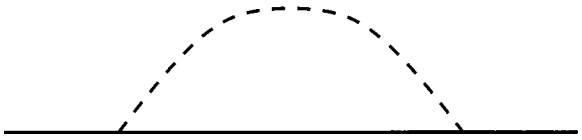

FIG. 6. Self-energy diagram for the fermion Green function. The solid (dashed) line is the fermion (gauge) propagator.

change k, the relative weight of the two broad peaks changes due to the k dependence of the coherence factors u and v. The mean-field results of the double-peak structure and the way in which the relative weight changes agree quite well with the numerical calculations.[31] However, the numerical calculations also observed certain shift of the positions of the two peaks as k changes. The mean-field results do not have this shift. If we include only the U term the peak positions in the renormalized electron spectral function still do not shift much. However, if we include both the U and $2t(\cos k_x + \cos k_y)$ terms the peak positions start to shift in a way similar to what is observed in numerical calculations, as has been pointed out by Laughlin in Ref. 30.

The electron spectral functions calculated above have pretty sharp peaks even at high energies (say for $\omega \approx -2J$) in contrast to experimental findings that quasiparticle peaks are much wider at high energies. This discrepancy can be resolved by including the self-energy of the fermion due to the gauge fluctuation. One can show that the self-energy from the diagram in Fig. 6 is proportional to ω and k. Thus the lifetime is proportional to the inverse of the quasiparticle energy. To include this effect, we may assume the electron Green function to have the form

$$G_e^{(0)} \simeq \frac{x}{2}\left[\frac{[v^f(k)]^2}{\omega - E_-^f(k) - i\gamma(\omega)} + \frac{[u^f(k)]^2}{\omega - E_+^f(k) - i\gamma(\omega)}\right] + G_{in}, \tag{66}$$

$$G_e = \frac{1}{(G_e^{(0)})^{-1} + U}. \tag{67}$$

If we assume the decay rate of the fermion to be $\gamma(\omega) = |\omega| + \gamma_0$, the resulting spectral function is quite similar to the line shapes observed in experiments.

To summarize, we have considered three models that treat different types of fluctuations. First is the locally condensed-boson picture. In this picture the quasiparticle peaks obtain intrinsic linewidths and line shapes. Also, this picture allows us to recover the Fermi surface that has the Luttinger volume in the URVB phase and the Fermi-liquid phase. Second is the short-range attraction between the bosons and the fermions. Those interactions are mainly due to the a_0^ℓ gauge and $|\chi_{ij}|$ fluctuations, which stretch the Fermi points of mean-field Green function into Fermi segments. This attraction can also make the electron Green function satisfy the spectral weight sum rule of the t-J model. Third is the decay of fermions ($\gamma \propto \omega$) due to the gauge fluctuations. This effect broadens the quasiparticle peaks at high energies and makes the spectral function look quite similar to the ones observed in experiment.

VI. GAUGE FIELDS

We next investigate the low-lying excitations of the effective action. We first consider the URVB state. Starting from Eq. (39), it is natural to introduce the transverse component of the gauge fields $\vec{a}_i$ by the standard replacement

$$\partial_i \rightarrow \partial_i + i\vec{a}_i \cdot \vec{\tau} + ie\vec{A}_i. \tag{68}$$

Recall that in the U(1) case, transverse gauge field enforces the constraint that the sum of the fermion and boson current should vanish. Here the three components of the gauge field a_i^ℓ, $\ell = 1,2,3$ enforce the vanishing of the analogous τ^ℓ currents corresponding to the τ^ℓ density constraint given in Eq. (9). An important difference is that in the SU(2) formulation the external electromagnetic field couples only to the bosons because the physical electron density is given in terms of the boson density by Eq. (8), whereas in the U(1) formulation one is free to couple the $\vec{A}$ field to the boson or fermion, and the physical response function is the same after including the screening by the U(1) gauge field, leading to the Ioffe-Larkin combination rules. We shall see how these rules are recovered or modified in the SU(2) case.

In the URVB case, it is most convenient to rotate locally to the U(1) formulation as done in Eq. (27). For g_i slowly varying in space, we have

$$U_{ij}^{(0)} \rightarrow g_i^\dagger U_{ij}^{(0)} g_j = U_{ij}^{(0)} + i\chi_0(\partial_\alpha g_j^\dagger) g_j, \tag{69}$$

where $i = j + \alpha$. This is because $U_{ij}^{(0)}$ is invariant under any global rotation. The second term in Eq. (69) gives rise to the usual transformation property of SU(2) gauge fields:

$$\vec{a}_0' \cdot \vec{\tau} = g^\dagger \vec{a}_0 \cdot \vec{\tau} g + (\partial_0 g^\dagger) g, \quad \vec{a}_i' \cdot \vec{\tau} = g^\dagger \vec{a}_i \cdot \vec{\tau} g - i(\partial_i g^\dagger) g \tag{70}$$

after combining with Eq. (23). In the rotated frame, the fermion $\tilde{\psi}$ obeys the U(1) mean-field solution with a chemical potential that enforces the fermion density to be $1-x$. We can now expand to quadratic order in a_μ'. The effective Lagrangian takes the form

$$\begin{aligned}\mathcal{L}_{\text{eff}} = {} & \tilde{h}^\dagger(\partial_\tau + \vec{a}_0' \cdot \vec{\tau} + eA_0)\tilde{h} + \frac{1}{2m_b}|(\partial_i + i\vec{a_i'} \cdot \vec{\tau} + ieA_i)\tilde{h}|^2 \\ & - \mu \tilde{h}^\dagger \tilde{h} + D_1 m_b^{-1}(\tilde{h}^\dagger \tilde{h})^2 \\ & + \frac{1}{2} a_\mu'^{\ell}(q,\omega_n) a_\nu'^{m}(-q,-\omega_n) \pi_{\mu\nu}^{\ell m}(q,\omega),\end{aligned} \tag{71}$$

where $\tilde{h} = (b,0)$,

$$\pi_{\mu\nu}^{\ell m}(q,\omega) = \langle j_\mu^\ell(q,\omega_n) j_\nu^m(-q,-\omega_n)\rangle, \tag{72}$$

$$j_0^\ell = \tilde{\psi}^\dagger \tau^\ell \tilde{\psi}, \tag{73}$$

$$j_\alpha^\ell = i[\tilde{\psi}^\dagger \tau^\ell \partial_\alpha \tilde{\psi} - (\partial_\alpha \tilde{\psi}^\dagger)\tau^\ell \tilde{\psi}]. \tag{74}$$

The spatial components are purely transverse

$$\pi_{\mu\nu}^{\ell m} = \left(\delta_{\mu\nu} - \frac{q_\mu q_\nu}{q^2}\right)\pi_\perp^{\ell m}(q,\omega) \tag{75}$$

and in the URVB state $\pi_\perp^{\ell m}=\delta_{\ell m}\pi_\perp$. This gives rise to three degenerate transverse gauge modes that are massless in the URVB state. This is confirmed by explicit calculation in Appendix B. In the Fermi-liquid phase b is Bose condensed and these modes are massive due to the Anderson-Higgs mechanism.

It is now clear from Eq. (71) that only the component $a_\mu'^{(3)}$ is capable of screening the $\vec{A}$ field. Thus it is the component of the gauge field parallel to the quantization axis in the rotated frame that plays the role of the U(1) gauge field. Equation (71) becomes

$$\mathcal{L}_{\rm eff}=b^\dagger(\partial_\tau+a_0'^3+eA_0)b+\frac{1}{2m_b}|(\partial_i+a_i'^{(3)}+eA_i)b|^2 -\mu|b|^2+D_1m_b^{-1}|b|^4+\frac{1}{2m_b}[(a_i'^{(1)})^2+(a_i'^{(2)})^2]|b|^2 +\frac{1}{2}a_\mu'^{\ell}(q,\omega_n)a_\nu'^{\ell}(-q,-\omega_n)\pi_{\mu\nu}^{\ell}(q,\omega). \tag{76}$$

The coupling of the perpendicular components $\ell=1,2$ to b may be approximated by the expectation value of $\langle(a_i'^{\ell})^2\rangle|b|^2$, which simply renormalizes the chemical potential μ. The a_i^3 component can be integrated out and gives rise to the Ioffe-Larkin combination rule

$$(\pi_{\mu\nu})^{-1}=(\pi_{\mu\nu}^B)^{-1}+(\pi_{\mu\nu}^F)^{-1}, \tag{77}$$

where π^F is the $\ell=3$ component, i.e., the usual density-density response function of the fermions. Equation (76) also shows that even in the SU(2) formulation, only a single component of the gauge field couples to the boson phase and plays an important role in suppressing the phase coherence of the boson, just as in the U(1) theory.

We next turn our attention to the s-flux phase. The main difference is that the U_{ij}^0 matrix is invariant only under a τ_3 rotation $g_i=\exp(i\theta\tau_3)$, so that the SU(2) symmetry is broken down to U(1). This produces a mass in the $\ell=1,2$ modes and only the $\ell=3$ gauge mode remains massless. This is also checked by explicit calculation in Appendix B. Phenomenologically, we are led to the following effective Lagrangian by gauging Eq. (52) and keeping only the a_μ^3 component of the gauge field:

$$\mathcal{L}_{\rm eff}=\frac{2m_b}{D_1}|z^\dagger D_0 z|^2+ixz^\dagger D_0 z-\frac{x}{2m_b}|D_i z|^2-\frac{4x^2\tilde{J}}{2C_1}|z_1z_2|^2 -\frac{x^2\tilde{J}}{2C_3}(|z_1|^2-|z_2|^2)^2+\frac{1}{2}a_\mu^3\pi^{\mu\nu}a_\nu^3, \tag{78}$$

where $\pi^{\mu\nu}$ is the polarization tensor of the fermions for a_μ^3 gauge field and $D_0=\partial_\tau+eA_0+a_0^3\tau^3$ and $D_i=\partial_i+ieA_i+ia_i^3\tau^3$.

Equation (78) describes the low-lying excitations of the underdoped regime: The superconducting and the spin-gap phases correspond to the ordered and thermally disordered phases of $\mathcal{L}_{\rm eff}$, respectively. We defer a full discussion of this problem to the future. Here we give a qualitative discussion of the superfluid density in the low-temperature phase. We integrate out a_μ^3 in the standard way and we find the following dependence of the transverse electromagnetic field $\vec{A}_i$:

$$\mathcal{L}_{\rm eff}=(eA_i)^2\frac{x}{m_b}\left[1-\frac{(z^\dagger\tau^3 z)^2}{1+m_b\pi_\perp/x}\right], \tag{79}$$

where $\pi^{ij}=\pi_\perp(\delta_{ij}-q_iq_j/q^2)$. The coefficient of A_i^2 is the superfluid density. On the minimum energy manifold $|z_1|=|z_2|$ the second term in Eq. (79) vanishes and the superfluid density is exactly x. This is the d-wave state as we discussed earlier. On the other hand, when the vector $\vec{I}$ points towards the north or south pole, $|z_1z_2|=0$ and we have $z^\dagger\tau^3z=\pm1$. In this case the fermion spectrum is that of the staggered-flux phase with a finite chemical potential. The response $\pi^{\mu\nu}$ for this orientation of $\vec{I}$ is that of a metal, which vanishes in the limit $\omega,q\to0,\omega<q$. In this case the two terms in Eq. (79) cancel and we find that $\rho_s=0$, i.e., the staggered-flux phase is not a superfluid. In general, we expect that in the superconducting phase fluctuations of $\vec{I}$ away from the equator will cause a reduction of the superfluid density due to the second term of Eq. (79). For a more complete treatment, we will need more detailed information on $\pi^{\mu\nu}$ and its dependence on $\vec{I}$, which will be discussed elsewhere.

VII. CONCLUSION

The main result of this paper is the derivation of the effective low-energy Lagrangian in terms of the boson fields z_1 and z_2 and their coupling to gauge fields. These are given in Eq. (39) together with Eq. (68) for the URVB and Fermi liquid phases and Eq. (78) for the s-flux and underdoped superconducting phases. In the case of the URVB phase and the Fermi liquid phase, we show that the σ-model approach allows a smooth crossover to the U(1) mean-field description, recovering all the desirable properties such as the Luttinger theorem for the Fermi surface area and the Ioffe-Larkin combination rules. This is a considerable improvement over the SU(2) mean-field theory.

In the staggered-flux phase the σ-model description offers some insight into the connection of the SU(2) with the U(1) theory. The staggered-flux phase is the disordered phase of the effective Lagrangian (78) so that we may interpret the spin-gap phase as fluctuations among d-wave state and s-flux states and a variety of states in between. While the phase diagram is quite similar to the U(1) theory, the collective excitations are very different. In the U(1) theory the gauge mode acquires a large mass gap of order $(1-x)J$. In the SU(2) theory there are three gauge modes, two are massive with mass of order Δ, while one remains massless. We believe the low-lying gauge modes may help stabilize this phase. In any case, the massless gauge modes will lead to large fluctuation effects, which we have not truly explored in this paper.

We also performed extensive numerical work to explore the consequence of the σ-model description for photoemission experiments. We find that within the uncertainties of the theory the qualitative features are not that different from the SU(2) mean-field theory once the boson-fermion attraction

was included. We find an energy gap in the electron spectrum, large near $(0,\pi)$ and vanishing along a Fermi segment near $(\pi/2,\pi/2)$. The precise size and location of these segments is beyond the accuracy of the present theory, but the $\vec{k}$ dependence is that of a broadened d-wave gap. We consider the agreement of this feature with the experiment to be strong support of the present approach. The SU(2) theory naturally describes an unusual superconducting transition that is not associated with opening or closing of spin gap. We have not treated gauge fluctuations adequately in this paper for us to describe the energy dependence or the line shape of the spectral function, so that at present detailed questions that distinguish the energy gap as measured from the leading edge or from the ''centroid'' of the spectral feature remain unanswered.

We expect the SU(2) mean-field theory to be applicable at high temperatures and the σ-model description to be more accurate near the phase boundary to the superconducting and the Fermi-liquid phases. This is because the fermions respond to local fluctuations in the boson fields on a length scale of $\xi_F=J/T$ in the URVB phase and $\xi_F=J/\Delta$ in the s-flux phase. On the other hand, the boson fluctuations are on a scale $\xi_B=(t/T)^{1/2}$ for $T>T_{BE}^{(0)}$ and $\xi_B=x^{-1/2}$ for $T<T_{BE}^{(0)}$, where $T_{BE}^{(0)}=\pi x t$ is a mean-field Bose-condensation temperature. When $\xi_F>\xi_B$, we expect the fermion to average over the local boson fluctuations and the SU(2) mean-field theory is appropriate, whereas the σ-model approach requires that $\xi_F<\xi_B$. The difficulty is that for $T<T_{BE}^{(0)}$ we do not have a good understanding of ξ_B because the coherence of the bosons is greatly suppressed by gauge fluctuations. In principle, we should solve the σ model to obtain ξ_B to obtain a self-consistent solution, but that is beyond the scope of the present paper. This is why we explore the consequences of both methods and it is fortunate that the results are qualitatively similar in the s-flux phase.

One important outcome of the present work is that it is clear that the transition to the superconducting state is very different from the conventional BCS theory. In BCS theory T_c is controlled by the closing of an energy gap in the electronic excitation spectrum. In the present case, T_c is controlled by boson fluctuations of our effective Lagrangian. We also note that the effective Lagrangian is not of the conventional Ginsburg-Landau form with a simple complex order parameter. The internal gauge degrees of freedom, parametrized by ϕ and θ [see Eq. (14)], plays an important role. For example, long range phase coherence can be destroyed by θ fluctuations. Thus our picture of the normal phase (the disordered phase of the σ model) is very different from that suggested by a number of workers,[32–34] based on the idea of phase fluctuations or a conventional BCS order parameter. In the latter picture normal state transport is due to charge $2e$ collective modes, whereas we have charge e metallic carriers. We believe the absence of signatures of strong superconducting fluctuations in the normal state favors our point of view.

ACKNOWLEDGMENTS

We would like to thank R.B. Laughlin for sharing his unpublished results. We also would like to thank Z. X. Shen for many helpful discussions. P.A.L. was supported by NSF-MRSEC Grant No. DMR-94-00334 and X.G.W. was supported by NSF Grant No. DMR-94-11574 and the A.P. Sloan Foundation.

APPENDIX A: RELATION BETWEEN U(1) AND SU(2) THEORY

We start with the usual U(1) slave boson formalism where the operator $c_{i\sigma}^\dagger$ creating an electron with spin σ on site i is represented by the spinon (fermion) operator $f_{i\sigma}^\dagger$ and the holon (boson) operator b_i as

$$c_{i\sigma}^\dagger = f_{i\sigma}^\dagger b_i . \tag{A1}$$

The physical states satisfy the local constraint

$$\left(\sum_\sigma f_{i\sigma}^\dagger f_{i\sigma} + b_i^\dagger b_i - 1 \right) |\text{phys}\rangle = 0. \tag{A2}$$

Then the partition function Z of the t-J model is represented in terms of the functional integral as

$$Z = \int D\psi\, D\psi^\dagger Db\; Db^* DU\; Da_0 \exp\left(-\int_0^\beta L \right), \tag{A3}$$

with the Lagrangian L given by

$$\begin{aligned} L = & \frac{\tilde{J}}{2} \sum_{\langle ij \rangle} \text{Tr}[\, U_{ij}^\dagger U_{ij}] \\ & + \frac{1}{2} \sum_{i,j,\alpha} \psi_{i\alpha}^\dagger \left[\left(\partial_\tau + \sum_{a=1}^3 a_0^a \tau_a \right) \delta_{ij} + \tilde{J} U_{ij} \right] \psi_{j\alpha} \\ & + \sum_i b_i^\dagger (\partial_\tau - \mu + a_0^3) b_i - t \sum_{i,j} \chi_{ij} b_j^\dagger b_i \\ = & L_F + L_B . \end{aligned} \tag{A4}$$

where the first line is the Lagrangian L_F for the fermions and the second line is the contribution L_B from the doped holes. Here the SU(2) matrix U_{ij} has the spinon pairing order parameter Δ_{ij} and the hopping order parameter χ_{ij} as the matrix elements, i.e., $U_{ij}=\left[\begin{smallmatrix} -\chi_{ij}^* & \Delta_{ij}^* \\ \Delta_{ij} & \chi_{ij} \end{smallmatrix}\right]$. The spinor $\psi_{i\alpha}$ is given by Eq. (1). We have introduced three a_0's. The three-component a_0^3 is the time component of the U(1) gauge field corresponding to the constraint (A2). The components 1 and 2 correspond to the constraint

$$\langle \text{phys}' | f_{i1} f_{i2} | \text{phys} \rangle = \langle \text{phys}' | f_{i1}^\dagger f_{i2}^\dagger | \text{phys} \rangle = 0, \tag{A5}$$

which are redundant[27] and are left out in the usual U(1) formulation.

Now we consider the SU(2) gauge transformation, which is defined as the rotation of the spinor ψ_i in terms of a SU(2) matrix g_i as

$$\psi_i \rightarrow \tilde{\psi}_i = g_i^\dagger \psi_i , \quad U_{ij} \rightarrow \tilde{U}_{ij} = g_i^\dagger U_{ij} g_j ,$$

$$\mathbf{a}_0 = \sum_{a=1}^3 a_0^a \tau_a \rightarrow \tilde{\mathbf{a}}_0 = g_i^\dagger \mathbf{a}_0 g_i - (\partial_\tau g_i^\dagger) g_i . \tag{A6}$$

The Lagrangian L_F for the fermions remains invariant with respect to the gauge transformation (A6), while the holon contribution L_B changes. Then away from the half filling, $(U,\mathbf{a}_0)$ and $(\widetilde{U},\widetilde{\mathbf{a}}_0)$ are physically different configurations. Next we divide the functional integral over U and $\mathbf{a}_0$ into two parts, i.e., the representative $(U^{(0)},\mathbf{a}_0^{(0)})$ and those that are related to it by the SU(2) rotation g as $g^\dagger U^{(0)} g$ and $\mathbf{a}_0 = g_i^\dagger \mathbf{a}_0^{(0)} g_i - (\partial_\tau g_i^\dagger) g_i$:

$$\int DU\, D\mathbf{a}_0 F(U,\mathbf{a}_0) = \int DU^{(0)} D\mathbf{a}_0^{(0)} \int Dg\; F(g^\dagger U^{(0)} g, g_i^\dagger \mathbf{a}_0^{(0)} g_i - (\partial_\tau g_i^\dagger) g_i). \tag{A7}$$

No two members of $(U^{(0)},\mathbf{a}_0^{(0)})$ are related by any SU(2) rotation g. We change the notation of the Grassmann variable in Eq. (A3) to $\widetilde{\psi}$ and then we change the Grassmann integral variables to $\psi = g\widetilde{\psi}$, $\psi^\dagger = \widetilde{\psi}^\dagger g^\dagger$ to obtain

$$Z = \int D\psi\, D\psi^\dagger Db\, Db^* DU^{(0)} D\mathbf{a}_0^{(0)} Dg \times \exp\left[-\int_0^\beta d\tau L'(\psi,\psi^\dagger,b,b^*,U^{(0)},\mathbf{a}_0^{(0)},g)\right]. \tag{A8}$$

The Lagrangian is given by

$$L' = \frac{\widetilde{J}}{2}\sum_{\langle i,j\rangle} \mathrm{Tr}(U_{ij}^\dagger U_{ij}) + \frac{1}{2}\sum_{i,j,\alpha} \psi_{i\alpha}^\dagger [(\partial_\tau + \mathbf{a}_0^{(0)})\delta_{ij} + \widetilde{J} U_{ij}^{(0)}]\psi_{j\alpha} + \sum_{i,j} b_i^* \left[\left(\partial_\tau - \mu + \frac{1}{2}\mathrm{Tr}\{\tau_3 [g_i^\dagger \mathbf{a}_0^{(0)} g_i - (\partial_\tau g_i^\dagger) g_i]\}\right)\delta_{ij} - \frac{t}{2}\mathrm{Tr}[(1+\tau_3) g_i^\dagger U_{ij}^{(0)} g_j]\right] b_j. \tag{A9}$$

We now parametrize g_i in terms of z_i using Eq. (13) and bind the z with the slave boson b to define the SU(2) boson $h = (b_1/b_2)$ as

$$b_{i\alpha} = z_{i\alpha} b_i. \tag{A10}$$

This can be represented by

$$h_i = g_i \begin{bmatrix} b_i \\ 0 \end{bmatrix}. \tag{A11}$$

Now the Lagrangian L' in Eq. (A9) is written in terms of b_1 and b_2 instead of b and g. First the Berry phase term is

$$\sum_i \left[b_i^* \partial_\tau b_i - \frac{1}{2}\mathrm{Tr}[\tau_3 (\partial_\tau g_i^\dagger) g_i] b_i^* b_i \right] = \sum_i \left[b_i^* \partial_\tau b_i + \frac{1}{2}\left(\sum_\alpha (z_{i\alpha}^* \partial_\tau z_{i\alpha} - z_{i\alpha} \partial_\tau z_{i\alpha}^*) b_i^* b_i \right)\right] = \sum_i \left[b_i^* \partial_\tau b_i + \sum_\alpha z_{i\alpha}^* \partial_\tau z_{i\alpha} b_i^* b_i \right] = \sum_{i,\alpha} b_{i\alpha}^* \partial_\tau b_{i\alpha}, \tag{A12}$$

where we have used the relation $\Sigma_\alpha z_\alpha^* z_\alpha = 1$ and $\partial_\tau(\Sigma_\alpha z_\alpha^* z_\alpha) = \Sigma_\alpha (z_\alpha \partial_\tau z_\alpha^* + z_\alpha^* \partial_\tau z_\alpha) = 0$. Next the hopping term of the boson is written as

$$-\frac{t}{2}\mathrm{Tr}[(1+\tau_3) g_i^\dagger U_{ij}^{(0)} g_j] b_i^* b_j = -t h_i^\dagger U_{ij}^{(0)} h_j. \tag{A13}$$

In summary, the partition function Z is written as

$$Z = \int D\psi\, D\psi^\dagger Dh\, Dh^\dagger DU^{(0)} D\mathbf{a}_0^{(0)} \exp\left(-\int_0^\beta \widetilde{L}\right), \tag{A14}$$

with the Lagrangian $\widetilde{L}$ given by

$$\widetilde{L} = \frac{\widetilde{J}}{2}\sum_{\langle i,j\rangle} \mathrm{Tr}[U_{ij}^{(0)\dagger} U_{ij}^{(0)}] + \frac{1}{2}\sum_{i,j,\alpha} \psi_{i\alpha}^\dagger [(\partial_\tau + \mathbf{a}_0^{(0)})\delta_{ij} + \widetilde{J} U_{ij}^{(0)}]\psi_{j\alpha} + \sum_i h_i^\dagger (\partial_\tau - \mu + \mathbf{a}_0^{(0)}) h_i - t\sum_{i,j} h_i^\dagger U_{ij}^{(0)} h_j. \tag{A15}$$

Now the Lagrangian is invariant with respect to the SU(2) gauge transformation given in Eq. (11). Then the constraint that no two configurations $(U^{(0)},\mathbf{a}_0^{(0)})$ are related by g can be relaxed because it gives only the constant gauge volume. Then we can drop (0) from U and $\mathbf{a}_0$. This has the form of the SU(2) gauge theory proposed by Wen and Lee. However, we note that in the latter theory, the last term in Eq. (A15) is replaced by $\widetilde{t}\Sigma_{ij} h_i^\dagger U_{ij}^{(0)} h_j$, where $\widetilde{t} = t/2$. A possible source of this difficulty is that in Eq. (A4) we impose three constraints using three Lagrangian multipliers a_0^a, whereas in the standard U(1) formulation, only a single Lagrangian multiplier a_0 is used. We cannot justify this procedure because the three constraints involve noncommuting operators. Another possible source of discrepancy is that in going from integration over b and g to integration over h, a Jacobian may be necessary.

APPENDIX B: MICROSCOPIC DERIVATION OF GAUGE FIELDS

In this appendix we describe the microscopic derivation of the gauge fields in each of the mean-field states. We begin by giving several arguments for when the gauge field is expected to be massless. We then show by explicit calculation that for the URVB phase there are three massless transverse gauge fields. Finally, we present a calculation of the propagator of the massless gauge field in the s-flux phase after integrating out the fermions. Because we are interested in the

low-energy dynamics, we consider only the massless gauge fields. The first task is to identify the massless gauge fields. For this purpose let us consider the following gauge-invariant term that appears in the free energy:[35]

$$F=\mathrm{Tr}(P_{ij,\ldots,k}U_{ii'}P^{\dagger}_{i'j',\ldots,k'}U_{i'i}), \tag{B1}$$

where

$$P_{ij,\ldots,k}=U_{ij}U_{jl}\cdots U_{mk}U_{ki} \tag{B2}$$

is the product of U's along a closed loop $i\rightarrow j\rightarrow\cdots\rightarrow$k$\rightarrow$i. When we write U_{ij} as

$$U_{ij}=U^{(0)}_{ij}e^{i\mathbf{a}_{ij}}=U^{(0)}_{ij}e^{ia^{a}_{ij}\tau_a}, \tag{B3}$$

with $U^{(0)}_{ij}$ the mean-field configuration, we obtain the following contribution to the free energy of a^{a}_{ij}:

$$\begin{aligned}\delta F&=\mathrm{Tr}(P^{(0)}_{ij,\ldots,k}U^{(0)}_{ii'}e^{ia^{a}_{ii'}\tau_a}P^{(0)\dagger}_{i'j',\ldots,k'}e^{-ia^{a}_{ii'}\tau_a}U^{(0)}_{i'i})\\&=\mathrm{Tr}(U^{(0)}_{i'i}P^{(0)}_{ij,\ldots,k}U^{(0)}_{ii'}e^{ia^{a}_{ii'}\tau_a}P^{(0)\dagger}_{i'j',\ldots,k'}e^{-ia^{a}_{ii'}\tau_a}).\end{aligned} \tag{B4}$$

Then if $P^{(0)}$ does not commute with τ_a, Eq. (B4) gives the mass to the gauge field a^a. For example, if $P^{(0)}=c_0 1+c_3\tau_3$, with c's being constants,

$$\begin{aligned}e^{i\mathbf{a}}P^{(0)}e^{-i\mathbf{a}}&=P^{(0)}+i[\mathbf{a},P^{(0)}]+\frac{1}{2}i^2[\mathbf{a},[\mathbf{a},P^{(0)}]]+\cdots\\&=c_0 1+c_3\tau_3+c_3(a^1\tau_2-a^2\tau_1)\\&\quad-\frac{c_3}{2}[(a^1)^2+(a^2)^2]\tau_3+\cdots,\end{aligned} \tag{B5}$$

and a^1 and a^2 becomes massive. This is nothing but the Higgs mechanism, where P is the Higgs field that is site variable belonging to the adjoint (vector) representation of SU(2). The condensation of P breaks the symmetry from SU(2) to U(1) and only one gauge field, i.e., a^3 in the above example, remains massless. On the other hand, if $P^{(0)}=c_0 1$ for every elementary plaquette, $P^{(0)}$ for arbitrary closed loop is const $\times$ 1 independent of the gauge choice. In this case we can choose a gauge where $U^{(0)}_{ij}\propto 1$ and all the gauge fields a^1,a^2,a^3 remain massless. Now we apply the general consideration above to the each mean-field state. We chose the gauge where the link variable $U^{(0)}_{ij}$ for each state is given by

$$U^{(0)}_{ii+x}=U^{(0)}_{ii+y}=i\chi_0 1 \tag{B6}$$

for the URVB state, while

$$\begin{aligned}U^{(0)}_{ii+x}&=-\chi\tau_3-i(-1)^{i_x+i_y}\Delta,\\U^{(0)}_{ii+y}&=-\chi\tau_3+i(-1)^{i_x+i_y}\Delta\end{aligned} \tag{B7}$$

for s-flux and π-flux states. Then the product of U's along an elementary plaquette $P^{(0)}_{\mathrm{pl}}$ is obtained as

$$P^{(0)}_{\mathrm{pl}}=\chi_0^4 1 \tag{B8}$$

for URVB state, and

$$P^{(0)}_{\mathrm{pl}}=[(\chi^2-\Delta^2)^2-4\chi^2\Delta^2]1\pm 4i\chi\Delta(\chi^2-\Delta^2)\tau_3 \tag{B9}$$

for s-flux and π-flux states. Then it can be easily seen that in URVB and π-flux ($\chi=\Delta$) states, all the gauge fields remain massless while only a^3 remains massless in the s-flux state. For the π-flux state we can choose the gauge where

$$U^{(0)}_{ii+x}=i(-1)^{i_y}\chi 1,\quad U^{(0)}_{ii+y}=i\chi 1. \tag{B10}$$

Now we explicitly derive the effective action for the gauge fields up to the quadratic orders. We start from the Lagrangian in Eq. (6). We divide the link variable U_{ij} and $\mathbf{a}_0$ into the mean-field value and the fluctuation around it

$$U_{ij}=U^{(0)}_{ij}+\delta U_{ij},\quad \mathbf{a}_0=\mathbf{a}^{(0)}_0+\delta\mathbf{a}_0. \tag{B11}$$

Integrating out the fermions and bosons, we obtain the effective action for δU_{ij} and $\delta\mathbf{a}_0$,

$$\begin{aligned}S_{\mathrm{eff}}=\tilde{J}\sum_{\langle i,j\rangle}\mathrm{Tr}[(U^{(0)\dagger}_{ij}+\delta U^{\dagger}_{ij})(U^{(0)}_{ij}+\delta U_{ij})]-\mathrm{Tr}_F\ln(-G^{-1}_{F0}\\+\delta\mathbf{a}_0+\tilde{J}\,\delta U_{ij})+\mathrm{Tr}_B\ln(-G^{-1}_{B0}+\delta\mathbf{a}_0+t\,\delta U_{ij}),\end{aligned} \tag{B12}$$

where $\tilde{J}=3J/8$ and Tr_F and Tr_B are the fermionic and bosonic traces. The Green functions G_{F0} and G_{B0} in the mean-field state are given by

$$G^{-1}_{F0}=i\omega_n-\mathbf{a}^{(0)}_0-\tilde{J}U^{(0)}_{ij},\quad G^{-1}_{B0}=i\omega_l-\mu_B-\mathbf{a}^{(0)}_0-tU^{(0)}_{ij}. \tag{B13}$$

Now we can expand Eq. (B12) as

$$\begin{aligned}S_{\mathrm{eff}}&=S_0+S_1+S_2+\cdots=\tilde{J}\sum_{\langle i,j\rangle}\mathrm{Tr}[U^{(0)\dagger}_{ij}U^{(0)}_{ij}]\\&\quad+\tilde{J}\sum_{\langle i,j\rangle}\mathrm{Tr}[U^{(0)\dagger}_{ij}\delta U_{ij}+\delta U^{\dagger}_{ij}U^{(0)}_{ij}]\\&\quad+\mathrm{Tr}[G_{F0}(\delta\mathbf{a}_0+\tilde{J}\,\delta U_{ij})]\\&\quad-\mathrm{Tr}[G_{B0}(\delta\mathbf{a}_0+t\,\delta U_{ij})]+\tilde{J}\sum_{\langle i,j\rangle}\mathrm{Tr}[\delta U^{\dagger}_{ij}\delta U_{ij}]\\&\quad+\frac{1}{2}\mathrm{Tr}_F[G_{F0}(\delta\mathbf{a}_0+\tilde{J}\,\delta U_{ij})G_{F0}(\delta\mathbf{a}_0+\tilde{J}\,\delta U_{i'j'})]\\&\quad-\frac{1}{2}\mathrm{Tr}_B[G_{B0}(\delta\mathbf{a}_0+t\,\delta U_{ij})\\&\quad\times G_{B0}(\delta\mathbf{a}_0+t\,\delta U_{i'j'})]+\cdots.\end{aligned} \tag{B14}$$

The mean-field equation is obtained from the condition that the first-order terms in δU vanish [here we chose the form Eq. (B7) for the s- and π-flux states, but the mean-field equations obtained are valid also for the URVB state by setting $\Delta=0$ and $\chi=\chi_0$]:

$$\widetilde{J\chi}=\int_{-\pi}^{\pi}\frac{d^2k}{(2\pi)^2}\Bigg[\frac{\widetilde{J\chi}\gamma_k^2}{4E_k}[1-2f(2\widetilde{J}E_k)]+\frac{t\chi\gamma_k^2}{4E_k}[n(-\mu_B-2tE_k)-n(-\mu_B+2tE_k)]\Bigg],$$

$$\widetilde{J}\Delta=\int_{-\pi}^{\pi}\frac{d^2k}{(2\pi)^2}\Bigg[\frac{\widetilde{J}\Delta\eta_k^2}{4E_k}[1-2f(2\widetilde{J}E_k)]+\frac{t\Delta\eta_k^2}{4E_k}[n(-\mu_B-2tE_k)-n(-\mu_B+2tE_k)]\Bigg], \tag{B15}$$

where

$$\gamma_k=\cos k_x+\cos k_y,\quad \eta_k=\cos k_x-\cos k_y,$$

$$E_k=\sqrt{(\chi\gamma_k)^2+(\delta\eta_k)^2}, \tag{B16}$$

and $f(x)$ and $n(x)$ are the Fermi and Bose distribution functions, respectively. The condition that the first-order terms in $\delta\mathbf{a}_0$ vanish gives Eq. (9), which is satisfied by the mean-field solutions.

Now we study the second-order terms S_2. From the considerations given above we consider only the gauge fields that commute with $P^{(0)}$. First consider the URVB and π-flux states, where $U_{ij}^{(0)}\propto 1$ and all the gauge fields remain massless. When we make a gauge transformation

$$U_{ij}^{(0)}\rightarrow U_{ij}=g_iU_{ij}^{(0)}g_j^{\dagger} \tag{B17}$$

the action does not change. Let us take $g_i=e^{i\theta_i\tau_a}$. If g_i commutes with $U_{ij}^{(0)}$, we have

$$U_{ij}=U_{ij}^{(0)}e^{i(\theta_i-\theta_j)\tau_a}. \tag{B18}$$

If we consider this as an expansion δU_{ij} about $U_{ij}^{(0)}$ which corresponds to a pure gauge configuration, we can see that the coefficient of the second-order term in $a_{ij}^a=\theta_i-\theta_j$ vanishes for any $a=1,2,3$ for the URVB and π-flux phases and only for $a=3$ for the s-flux phase.

Generally, the second-order contribution S_2 can be written as

$$S_2=\frac{1}{2}\sum_{a,b}\sum_{\mu,\nu}\sum_{q,i\omega_n}\Pi_{\mu\nu}^{ab}(q,i\omega_n)a_\mu^a(q,i\omega_n)a_\nu^b(-q,-i\omega_n) \tag{B19}$$

and the above consideration guarantees the masslessness of a^a and leads to the condition

$$\Pi_{\mu\nu}^{ab}(q=0,i\omega_n=0)=0. \tag{B20}$$

Here $a,b=1,2,3$ for the URVB and π-flux states, while $a=b=3$ for the s-flux state.

To make things more clear, we describe here the explicit calculation for the URVB state. Taking the gauge choice of Eq. (B6), the mean-field equation is obtained as

$$\widetilde{J\chi}_0=\frac{1}{2}\int_{-\pi}^{\pi}\frac{d^2k}{(2\pi)^2}[\widetilde{J}\widetilde{\gamma}_kf(-2\widetilde{J\chi}_0\widetilde{\gamma}_k)+t\widetilde{\gamma}_kn(-\mu_B-2t\chi_0\widetilde{\gamma}_k)], \tag{B21}$$

where $\widetilde{\gamma}_k=\sin k_x+\sin k_y$. At first glance this appears different from Eq. (B15), but it can be shown by using partial integration that Eq. (B15) is reduced to Eq. (B21) by setting $\Delta=0$ and $\chi=\chi_0$. This can be also written as

$$\widetilde{J\chi}_0=-\int_{-\pi}^{\pi}\frac{d^2k}{(2\pi)^2}[\widetilde{J}^2\chi_0\widetilde{\gamma}_k^2f'(-2\widetilde{J\chi}_0\widetilde{\gamma}_k)+t^2\chi_0\widetilde{\gamma}_k^2n'(-\mu_B-2t\chi_0\widetilde{\gamma}_k)], \tag{B22}$$

where $f'(x)=\partial f(x)/\partial x[n'(x)=\partial n(x)/\partial x]$.

Now we consider the second-order contribution S_2. The gauge fields are related to δU_{ij} as

$$\delta U_{ii+\mu}=\delta U_{ii+\mu}^{\dagger}=-\chi_0a_{ii+\mu}^a\tau_a. \tag{B23}$$

Then the coupling $S_{\rm int}$ between the fermions (bosons) with the gauge field is written as

$$S_{\rm int}=-\frac{1}{\sqrt{\beta N}}\sum_{a,\mu,\nu}\sum_{k,q}\cos k_\mu[2\widetilde{J\chi}_0a_\mu^a(q)\psi_{k+q/2}\tau_a\psi_{k-q/2}+2t\chi_0a_\mu^a(q)h_{k+q/2}\tau_ah_{k-q/2}], \tag{B24}$$

where $\psi,\psi^{\dagger}$ are spinors. Now S_2 is explicitly given by

$$S_2=\sum_{a,\mu,\nu}\sum_q[2\widetilde{J\chi}_0^2\delta_{\mu\nu}-\Pi_{\mu\nu}^{Fab}(q)-\Pi_{\mu\nu}^{Bab}(q)]a_\mu^a(q)a_\nu^b\times(-q), \tag{B25}$$

where

$$\Pi_{\mu\nu}^{Fab}(q)=4\delta_{ab}\widetilde{J}^2\chi_0^2\int_{-\pi}^{\pi}\frac{d^2k}{(2\pi)^2}\cos k_\mu\times\cos k_\nu\frac{f(\xi_{k+q/2})-f(\xi_{k-q/2})}{i\omega_m-\xi_{k+q/2}+\xi_{k-q/2}}, \tag{B26}$$

where $\xi_k=-2\widetilde{J\chi}_0\widetilde{\gamma}_k$. A similar expression is obtained for $\Pi_{\mu\nu}^{Bab}(q)$. It can be easily seen that in the limit $q\rightarrow 0$, $\Pi_{\mu\nu}^{Fab}(q)+\Pi_{\mu\nu}^{Bab}(q)\rightarrow 2\widetilde{J\chi}_0^2\delta_{\mu\nu}$ by using the mean-field equation (B22). A similar cancellation is obtained for a^1,a^2,a^3 in the π-flux state and for a^3 in the s-flux state.

Finally, we present a calculation of the gauge field propagator when the fermions are integrated out, i.e., we compute $\Pi_{\mu\nu}^{Fab}(q,i\omega_n)=\Pi_{\mu\nu}^{Fab}(q,i\omega_n)-\Pi_{\mu\nu}^{Fab}(q=0,i\omega_n=0)$ in terms of the continuum approximation in the limit of small v_Fq,ω_n, and T compared with J. For the URVB state, this calculation is exactly the same as in the U(1) case described in Ref. 10. For the s-flux state, we consider the following effective Lagrangian for the fermions in the continuum approximation:

$$L=\int d^2r\ \psi_1^\dagger[D_\tau-2i\tilde{J}\tilde{\chi}(D_x+D_y)\sigma_3\tau_3 +i2\tilde{J}\Delta(D_x-D_y)\sigma_2]\psi_1 +\int d^2r\ \psi_2^\dagger[D_\tau-2i\tilde{J}\tilde{\chi}(D_x-D_y)\sigma_3\tau_3+i2\tilde{J}\Delta(D_x +D_y)\sigma_2]\psi_2, \tag{B27}$$

where $D_\mu=\partial_\mu+i\tilde{a}_\mu^3$. Since the problem has relativistic symmetry, it is convenient to introduce $\tilde{a}_\mu=(-ia_0,a_x,a_y)$. The spinor ψ_1 [ψ_2] describes the fermions near $\pm(\pi/2,\pi/2)$ [$\pm(\pi/2,-\pi/2)$] in k space. Because of the double periodicity in the gauge choice of Eq. (B7), k and $k+(\pi,\pi)$ are coupled and σ's are the Pauli matrices describing this 2×2 space in addition to the original isospin space spanned by τ matrices. When we integrated over the fermions in Eq. (B27), the following integral $g_{\mu\nu}(\mathbf{q})$ appears:

$$g_{\mu\nu}(\mathbf{q})=\int\frac{d^3k}{(2\pi)^3}\frac{k_\mu(\mathbf{k}+\mathbf{q})_\nu}{\mathbf{k}^2(\mathbf{k}+\mathbf{q})^2}, \tag{B28}$$

where $\mathbf{k}=(k_0,k_1,k_2)=(\omega,\vec{k})$ is the vector in 2+1 dimensions.

By using Feynman's trick, i.e.,

$$\frac{1}{ab}=\int_0^1\frac{dz}{[az+b(1-z)]^2}, \tag{B29}$$

the integral is transformed as

$$g_{\mu\nu}(\mathbf{q})==\int_0^1dz\int\frac{d^3k}{(2\pi)^3}\frac{k_\mu(\mathbf{k}+\mathbf{q})_\nu}{[(\mathbf{k}+z\mathbf{q})^2+z(1-z)\mathbf{q}^2]^2} =\int_0^1dz\int\frac{d^3k}{(2\pi)^3}\frac{k_\mu^2\delta_{\mu\nu}+z(1-z)q_\mu q_\nu}{[\mathbf{k}^2+z(1-z)q^2]^2}. \tag{B30}$$

Now $g_{\mu\mu}(q)$ is diverging if the ultraviolet cutoff Λ for k integration is infinity. This is cured if one considers $g_{\mu\nu}(q)-g_{\mu\nu}(0)$, which is converging when $\Lambda\to\infty$. Using

$$\int\frac{d^3k}{(2\pi)^3}\frac{1}{\mathbf{k}^2(\mathbf{k}+\mathbf{q})^2}=\frac{1}{8q},$$

where $q=\sqrt{\vec{q}^2+\omega^2}$, we obtain

$$g_{\mu\nu}(\mathbf{q})-g_{\mu\nu}(0)=\frac{q_\mu q_\nu-\delta_{\mu\nu}\mathbf{q}^2}{8q}\int_0^1dz\sqrt{z(1-z)} =\frac{q_\mu q_\nu-\delta_{\mu\nu}\mathbf{q}^2}{8q}. \tag{B31}$$

Using Eqs. (B31) and (B32), we obtain the effective action of the gauge field at zero temperature

$$S_{\rm eff}=\sum_{\mathbf{q}}\frac{1}{q}\Big[\tilde{J}^2\chi\Delta f_{xy}(\mathbf{q})f_{xy}(-\mathbf{q})+\frac{\chi^2+\Delta^2}{16\chi\Delta} \times[f_{0x}(\mathbf{q})f_{0x}(-\mathbf{q})+f_{0y}(\mathbf{q})f_{0y}(-\mathbf{q})]\Big], \tag{B32}$$

where $f_{\mu\nu}=\partial_\mu\tilde{a}_\nu-\partial_\nu\tilde{a}_\mu$. The coefficient of $a_\mu a_\nu$ of this expression gives the inverse of the gauge propagator that is correct for small q and ω in the lattice model.

APPENDIX C: ELECTRON SPECTRAL FUNCTION

The more exact expression of the mean-field electron Green function $G_e^{(0)}$ is given by

$$\begin{aligned}G_e^{(0)}&\equiv\langle T(c_\uparrow c_\uparrow^\dagger)\rangle\\ &=\frac{1}{N}\frac{1}{2}\sum_q[u^b(q-k)u^f(q)+v^b(q-k)v^f(q)]^2\\ &\times\sum_{\alpha=+,-}\{n_b[E_\alpha^b(q-k)]+n_F[E_\alpha^f(q)]\}\\ &\times\frac{1}{\omega-[E_\alpha^f(q)-E_\alpha^b(q-k)]-i\delta}+\frac{1}{N}\frac{1}{2}\\ &\times\sum_q[u^b(q-k)v^f(q)-v^b(q-k)u^f(q)]^2\\ &\times\sum_{\alpha=+,-}\{n_b[E_\alpha^b(q-k)]+n_F[E_{-\alpha}^f(q)]\}\\ &\times\frac{1}{\omega-[E_{-\alpha}^f(q)-E_\alpha^b(q-k)]-i\delta}.\end{aligned} \tag{C1}$$

Here N is the number of sites and

$$E_\pm^f(k)=\pm\sqrt{(\epsilon_k^f)^2+(\eta_k^f)^2},$$

$$\epsilon_k^f=2\tilde{J}\tilde{\chi}(\cos k_x+\cos k_y),$$

$$\eta_k^f=2\tilde{J}\Delta(\cos k_x-\cos k_y),$$

$$E_\pm^b(k)=\pm\sqrt{(\epsilon_k^b)^2+(\eta_k^b)^2}-\mu_B,$$

$$\epsilon_k^b=2\tilde{t}\tilde{\chi}(\cos k_x+\cos k_y),$$

$$\eta_k^f=2\tilde{t}\Delta(\cos k_x-\cos k_y),$$

$$u^{f,b}(k)=\frac{1}{\sqrt{2}}\sqrt{1+\frac{\epsilon_k^{f,b}}{\sqrt{(\epsilon_k^{f,b})^2+(\eta_k^{f,b})^2}}},$$

$$v^{f,b}(k)=\frac{1}{\sqrt{2}}\frac{\eta_k^{f,b}}{|\eta_k^{f,b}|}\sqrt{1-\frac{\epsilon_k^{f,b}}{\sqrt{(\epsilon_k^{f,b})^2+(\eta_k^{f,b})^2}}}.$$

$n_{b,f}(E)$ are boson or fermion occupation numbers at energy E. The incoherent part comes from the terms containing $n_f(E_\pm^f)$. One can show that $\mathrm{Im}G_{in}^{(0)}=0$ for $\omega>0$ and

$$\int\frac{d\omega}{2\pi}\mathrm{Im}G_{in}^{(0)}=\frac{1}{2}. \tag{C2}$$

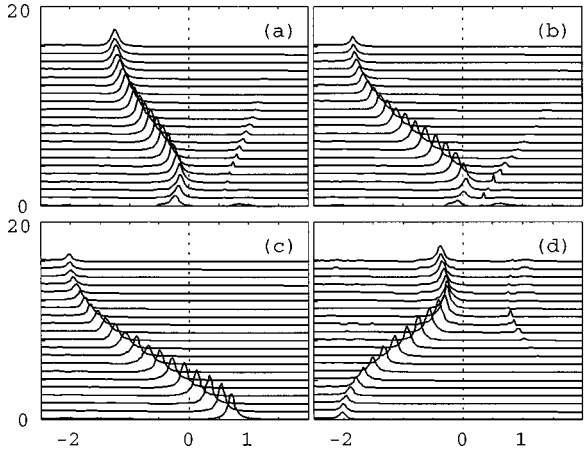

FIG. 7. Electron spectral function for $U_2/U_1=-1/3$. The curves are for the following values of k, from top to bottom: (a) $k=(-\pi/4,\pi/4)\rightarrow(\pi/4,3\pi/4)$, (b) $k=(-\pi/8,\pi/8)\rightarrow(3\pi/8,5\pi/8)$, (c) $k=(0,0)\rightarrow(\pi/2,\pi/2)$, and (d) $k=(0,\pi)\rightarrow(0,0)$. We have chosen $J=1$.

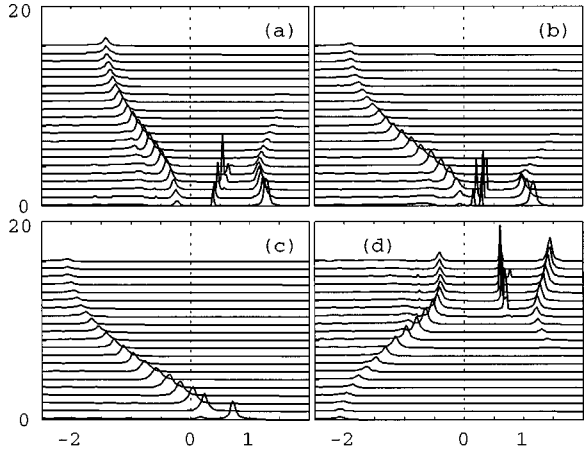

FIG. 8. Electron spectral function for $U_2/U_1=1$. The curves are for the following values of k, from top to bottom: (a) $k=(-\pi/4,\pi/4)\rightarrow(\pi/4,3\pi/4)$, (b) $k=(-\pi/8,\pi/8)\rightarrow(3\pi/8,5\pi/8)$, (c) $k=(0,0)\rightarrow(\pi/2,\pi/2)$, and (d) $k=(0,\pi)\rightarrow(0,0)$. We have chosen $J=1$.

The coherent parts come from the terms containing $n_b(E^b_-)$. Note that $n_b[E^b_-(k)]$ is almost zero except near $(0,0)$ and (π,π). Approximating those peaks by δ functions in k space, we get

$$G_e^{(0)}(k)\simeq\frac{x}{2}\left[\frac{[v^f(k)]^2}{\omega-E^f_-(k)}+\frac{[u^f(k)]^2}{\omega-E^f_+(k)}\right]+G_{in}. \quad \text{(C3)}$$

Next we will consider effects of fluctuations. We will consider two different types of fluctuations. The first one is the fluctuations of $a_0^{\swarrow}$ whose effect is modeled by the effective short-range interaction between the fermions and the bosons:

$$\psi^\dagger\vec{\tau}\psi h^\dagger\vec{\tau}h\ . \quad \text{(C4)}$$

The second one is the fluctuations of $|\chi_{ij}|$ that induces

$$-t(h^\dagger\psi)_i(\psi^\dagger h)_j=-2tc_ic_j^\dagger. \quad \text{(C5)}$$

In the s-flux phase the electron operator $c^\dagger=1/\sqrt{2}\psi^\dagger h$ mixes with an operator $\tilde{c}^\dagger=1/\sqrt{2}\psi^\dagger\tau^3 h$. We find that $\langle T\tilde{c}^\dagger_{k+Q}c_k\rangle\equiv iG_Q^{(0)}$ with $Q=(\pi,\pi)$ is nonzero and given by

$$\begin{aligned}G_Q^{(0)}(k)=&\frac{1}{N}\frac{1}{2}\sum_q\ [u^f(q)u^b(q-k)+v^f(q)v^b(q-k)]\\&\times[v^f(q)u^b(q-k)-u^f(q)v^b(q-k)]\\&\times\sum_{\alpha,\beta=+,-}\alpha\beta\{n_b[E^b_\beta(q-k)]+n_F[E^f_\alpha(q)]\}\\&\times\frac{1}{\omega-[E^f_\alpha(q)-E^b_\beta(q-k)]-i\delta} \quad \text{(C6)}\\\simeq&\frac{x}{2}v^f(k)u^f(k)\left(-\frac{1}{\omega-E^f_+(k)}+\frac{1}{\omega-E^f_-(k)}\right)+\tilde{G}_{in}. \quad \text{(C7)}\end{aligned}$$

Since the interaction couples to both c and $\tilde{c}$, we have to invert a 2×2 matrix to calculate the electron Green function. Noting that $\langle c_kc_k\rangle=\langle\tilde{c}^\dagger_k\tilde{c}^\dagger_k\rangle$ and introducing

$$\boldsymbol{G}=\begin{pmatrix}G_e^{(0)}(k) & -iG_Q^{(0)}(k)\\ G_Q^{(0)}(k) & G_e^{(0)}(k+Q)\end{pmatrix}, \quad \text{(C8)}$$

we find that the electron Green function is the (1,1) component of the 2×2 matrix

$$G_e=\left[\boldsymbol{G}^{-1}+\begin{pmatrix}U_1 & 0\\ 0 & U_2\end{pmatrix}\right]^{-1}_{11}. \quad \text{(C9)}$$

Note that when $U_2=0$ Eq. (C9) reduces to Eq. (60). $U_{1,2}$ are obtained by rewriting the interaction (C4) in the c and $\tilde{c}$ basis:

$$U\psi^\dagger\vec{\tau}\psi h^\dagger\vec{\tau}h=3Uc^\dagger c-U\frac{1}{2}\psi^\dagger\vec{\tau}hh^\dagger\vec{\tau}\psi \quad \text{(C10)}$$

$$=3Uc^\dagger c-U\tilde{c}^\dagger\tilde{c}+\cdots. \quad \text{(C11)}$$

The term represented by the ellipsis has the form $\psi^\dagger\tau^{1,2}hh^\dagger\tau^{1,2}\psi$ and does not contribute to the electron Green function. Thus $U_1=3U$ and $U_2=-U$ for the interaction in Eq. (C4).

At low energies the interactions are dressed by fermion bubbles. Because the a^3_μ gauge field is massless in the s-flux phase, its fluctuations mediate a long-range interaction. Thus the interaction $\psi^\dagger\tau^3\psi h^\dagger\tau^3h$ is enhanced at low energies. To study this effect let us consider an extreme case, which has the interaction

$$U\psi^\dagger\tau^3\psi h^\dagger\tau^3h \quad \text{(C12)}$$

$$=Uc^\dagger c+U\tilde{c}^\dagger\tilde{c}+\cdots. \quad \text{(C13)}$$

The term represented by the ellipsis does not contribute to the electron Green function. Thus the electron Green function in this case is given by Eq. (C9) with $U_1=U_2=U$.

From the above discussion, it is also easy to see that the interaction induced by the $|\chi_{ij}|$ fluctuations modifies only U_1:

$$G_e=\left[\boldsymbol{G}^{-1}+\begin{pmatrix} U_1+2t(\cos k_x+\cos k_y) & 0 \\ 0 & U_2 \end{pmatrix}\right]^{-1}_{11}. \tag{C14}$$

In summary, if we treat bosons as a free Bose gas and include the attraction induced by the gauge and $|\chi_{ij}|$ fluctuations, the electron Green function is approximately given by Eq. (C14). However, different treatments of fluctuations result in U_2/U_1 in a range from $-1/3$ to 1 and absolute magnitudes of $U_{1,2}$ are of order t.

In Figs. 7 and 8 we plot the electron spectral function for $U_2/U_1=-1/3,1$. We have chosen $\tilde{J}=J/2$, $\tilde{t}=t=2J$, $\chi=1$, $\Delta/\chi=0.4$, $x=0.1$, and $T=0.1J$. The value U_1 is determined from requiring the renormalized electron Green function to satisfies the sum rule

$$\int_0^\infty \frac{d\omega\ d^2k}{(2\pi)^3}\mathrm{Im}G_e=x. \tag{C15}$$

The main purpose of the above study is to understand the ambiguity in the electron spectral function due to our uncertainty in treating gauge fluctuation. We find that the gap near $(0\pm\pi)$ and $(\pm\pi,0)$ survives the inclusion of gauge fluctuation. However, spectral functions near $(\pm\pi/2,\pm\pi//2)$ are modified. For $\omega<0$ the electron spectral functions are quite similar for the three different choices of $U_2/U_1=-1/3,0,1$. However, for $\omega>0$ the spectral functions show some notable differences.

[1] B. O. Wells *et al.*, Phys. Rev. Lett. **74**, 964 (1995).
[2] See Z. X. Shen and D. S. Dessau, Phys. Rep. **253**, 1 (1995).
[3] P. W. Anderson, Science **235**, 1196 (1987).
[4] G. Baskaran, Z. Zou, and P. W. Anderson, Solid State Commun. **63**, 973 (1987).
[5] I. Affleck and J. B. Marston, Phys. Rev. B **37**, 3774 (1988).
[6] G. Kotliar and J. Liu, Phys. Rev. B **38**, 5142 (1988).
[7] Y. Suzumura, Y. Hasegawa, and H. Fukuyama, J. Phys. Soc. Jpn. **57**, 2768 (1988).
[8] G. Baskaran and P. W. Anderson, Phys. Rev. B **37**, 580 (1988).
[9] L. Ioffe and A. Larkin, Phys. Rev. B **39**, 8988 (1989).
[10] P. A. Lee and N. Nagaosa, Phys. Rev. B **46**, 5621 (1992).
[11] See A. J. Millis, L. Ioffe, and H. Monien, J. Phys. Chem. Solids **56**, 1641 (1995).
[12] J. W. Loram *et al.*, Physica C **235**, 134 (1994).
[13] C. C. Homes *et al.*, Phys. Rev. Lett. **71**, 1645 (1993); S. Uchida, K. Tamasaku, and S. Tajima, Phys. Rev. B **53**, 14 558 (1996).
[14] S. Uchida *et al.*, J. Low Temp. Phys. **105**, 723 (1996).
[15] D. N. Basov *et al.*, Phys. Rev. Lett. **77**, 4090 (1996).
[16] A. J. Millis and H. Monien, Phys. Rev. Lett. **70**, 2810 (1993).
[17] D. G. Marshall *et al.*, Phys. Rev. Lett. **76**, 4841 (1996).
[18] H. Ding *et al.*, Nature (London) **382**, 51 (1996).
[19] T. M. Rice, in *The Physics and Chemistry of Oxide Superconductors*, edited by Y. Iye and H. Yasuoka (Springer-Verlag, Berlin, 1992), p. 313.
[20] T. Tanamoto, K. Kohno, and H. Fukuyama, J. Phys. Soc. Jpn. **61**, 1886 (1992); H. Fukuyama, Prog. Theor. Phys. Suppl. **108**, 287 (1992).
[21] M. U. Ubbens and P. A. Lee, Phys. Rev. B **49**, 6853 (1994).
[22] R. Hlubina, W. Putikka, T. M. Rice, and D. Khveshchenko, Phys. Rev. B **46**, 11 224 (1992).
[23] L. Ioffe and A. J. Millis, Phys. Rev. B **54**, 3645 (1996).
[24] X.-G. Wen and P. A. Lee, Phys. Rev. Lett. **76**, 503 (1996).
[25] T. C. Hsu, Phys. Rev. B **41**, 11 379 (1990).
[26] R. B. Laughlin, J. Phys. Chem. Solids **56**, 1627 (1995).
[27] I. Affleck, Z. Zou, T. Hsu, and P. W. Anderson, Phys. Rev. B **38**, 745 (1988).
[28] The factor 3/8 in $\tilde{J}$ arises due to the simultaneous decoupling of the quartic fermion term in several channels. See M. Ubbens and P. Lee, Phys. Rev. B **46**, 8434 (1992), and references therein; The factor of 1/2 in $\tilde{t}$ arises from the factor $\sqrt{2}$ in Eq. (3) and was missed in Ref. 24.
[29] N. Nagaosa and P. Lee, Phys. Rev. B **45**, 966 (1992).
[30] R. B. Laughlin (unpublished).
[31] A. Moreo, S. Haas, A. Sandvik, and E. Dagotto, Phys. Rev. B **51**, 12 045 (1995).
[32] Y. Uemura *et al.*, Phys. Rev. Lett. **66**, 2665 (1991).
[33] V. Emery and S. Kivelson, Nature (London) **374**, 434 (1995).
[34] M. Randeria, N. Trivedi, A. Moreo, and R. Scalettar, Phys. Rev. Lett. **69**, 2001 (1992).
[35] X. G. Wen, Phys. Rev. B **44**, 2664 (1991).